

Theory of spin-polarized bipolar transport in magnetic p-n junctions.

Jaroslav Fabian

Institute for Theoretical Physics, Karl-Franzens University, Universitätsplatz 5, 8010 Graz, Austria

Igor Zutic and S. Das Sarma

Condensed Matter Theory Center, Department of Physics,
University of Maryland at College Park, College Park, Maryland 20742-4111, USA

The interplay between spin and charge transport in electrically and magnetically inhomogeneous semiconductor systems is investigated theoretically. In particular, the theory of spin-polarized bipolar transport in magnetic p-n junctions is formulated, generalizing the classic Shockley model. The theory assumes that in the depletion layer the nonequilibrium chemical potentials of spin up and spin down carriers are constant and carrier recombination and spin relaxation are inhibited. Under the general conditions of an applied bias and externally injected (source) spin, the model formulates analytically carrier and spin transport in magnetic p-n junctions at low bias. The evaluation of the carrier and spin densities at the depletion layer establishes the necessary boundary conditions for solving the diffusive transport equations in the bulk regions separately, thus greatly simplifying the problem. The carrier and spin density and current profiles in the bulk regions are calculated and the I-V characteristics of the junction are obtained. It is demonstrated that spin injection through the depletion layer of a magnetic p-n junction is not possible unless nonequilibrium spin accumulates in the bulk regions (either by external spin injection or by the application of a large bias). Implications of the theory for majority spin injection across the depletion layer, minority spin pumping and spin amplification, giant magnetoresistance, spin-voltaic effect, biasing electrode spin injection, and magnetic drift in the bulk regions are discussed in details, and illustrated using the example of a GaAs based magnetic p-n junction.

I. INTRODUCTION

Active control of spin in semiconductors¹ is projected to lead to significant technological advances, most importantly in digital information storage and processing, magnetic recording and sensing, and quantum computing.^{2,3} Using semiconductors for spintronic applications (where spin, in addition to charge, is manipulated to influence electronic properties) has several advantages. First, integration of spintronics with traditional semiconductor technology calls for employing semiconductors (rather than metals) as media for spin control. Second, semiconductors are versatile materials, not only for their electrical properties, but also for their spin/magnetic characteristics. Doping control of electrical and magnetic properties, optical spin orientation and detection, bipolar (electron and hole) transport, and interface properties (charge and spin accumulation and depletion) leading to device concepts from p-n junction diodes to field-effect transistors, are among the great advantages of semiconductors over other candidates for spintronic materials. By allowing for the active control and manipulation of carrier spin and charge by electric and magnetic fields as well as by light, semiconductor spintronics creates the potential for an integrated magneto-optoelectronics technology.

A generic semiconductor spintronics scheme involves three steps: injection of nonequilibrium spin into a semiconductor, spin storage, manipulation, and transfer, and spin detection. Spin injection was historically first accomplished optically, by illuminating a semiconductor with circularly polarized light (the so called spin orientation.⁴ Electrical spin injection (that is, spin injection from a magnetic electrode, often called simply spin injection) into semiconductors, while predicted theoretically already in the 70s,⁵ has been demonstrated only recently,⁶ and realized as an injection from a magnetic semiconductor,^{7,8,9} a ferromagnetic metal,^{10,11,12} and a ferromagnetic metal/tunnel barrier contact.^{13,14,15,16,17}

Once injected, nonequilibrium spin survives for a reasonably long time when compared to typical relaxation times of momentum and energy of the injected carriers. Room temperature spin relaxation times in semiconductors are typically nanoseconds^{4,18} (compared to sub picosecond time scales for momentum and energy relaxation). Similar in magnitude are only carrier (electron and hole) recombination times, which are usually between micro- to nanoseconds. If not in the ballistic regime, transport of spin in a semiconductor can be characterized as carrier recombination and spin relaxation limited drift and diffusion. Spin typically diffuses over micron distances from the point of injection, sufficient for microelectronics applications. Application of large electric fields can further drag the injected spin over several microns at low temperatures, as in intrinsic GaAs,¹⁹ and even up to 100 μm in n-doped GaAs.²⁰ (As far as the spin diffusion length is concerned, metals have an advantage: because of the large Fermi velocity, spin diffusion

lengths in metals can be as large as centimeters.) Important for device applications are studies of spin transport in inhomogeneous semiconductors. It has already been shown, for example, that spin phase can be preserved in transport across heterostructure interfaces,²¹ that electron spin can be controlled by bias in semimagnetic resonant tunneling diodes,²² and that spin can tunnel through the transition region of tunnel diodes.^{23,24} The final step of a generic spintronics scheme is spin detection. Traditionally, spin in semiconductors has been detected optically by observing circular polarization of the recombination light.⁴ Efforts to electrically detect nonequilibrium spin in semiconductors rely on spin-charge coupling, realized either as spin-dependent Schottky barrier transport^{25,26} or as magnetoresistance²⁷ and galvanovoltanic²⁸ effects.

After the discovery of ferromagnetism in III-V semiconductor compounds,^{29,30} the great push for semiconductor spintronics came with the fabrication of (Ga,Mn)As which is ferromagnetic above 100 K.^{31,32} Ferromagnetic semiconductors can not only serve to inject and detect spin in all-semiconductor spintronic devices, but can also form a basis for nonvolatile memory, opening prospects of integrated, single-chip memory and logic applications (feasibility of such prospects has been demonstrated by controlling semiconductor ferromagnetism optically^{33,34} and electrically³⁵). There is a steady increase in the number of available ferromagnetic semiconductors, including a first group-IV compound GeMn,³⁶ (In,Ga,Mn)As,³⁷ reported room temperature ferromagnets Mn-doped CdGeP₂,³⁸ GaN,³⁹ and GaP,⁴⁰ and Co-doped TiO₂.⁴¹

Closely following the experimental progress, many theoretical efforts have been dedicated to understanding electrical spin injection into semiconductors^{42,43,44,45,46,47,48} and investigating fundamental issues of spin-polarized transport in semiconductors.^{4,49,50,51,52,53,54,55,56,57} Another direction for fundamental spintronics theory has been predicting and analyzing various spintronics device architectures for possible technological³³ applications. The common goal of these studies is devising spin valves and structures (typically including one or several magnetic layers) with maximized magnetoresistance. To this end various spin field-effect transistors have been proposed,^{58,59,60} where the source and drain are ferromagnetic electrodes serving to inject and detect spin which is transported in a (typically) nonmagnetic channel. Spin and charge transport in the channel are controlled by gate bias through the Rashba effect.^{61,62} Other proposed spintronics device schemes include heterostructure spin filters^{63,64,65,66,67,68,69,70,71,72} and spin polarization detectors,⁷³ resonant tunneling diodes,⁷⁴ unipolar magnetic diodes,⁷⁵ quantum interference mesoscopic schemes^{76,77,78} and various spin emitters.^{28,79,80,81,82,83}

We have recently proposed two spintronics device schemes that take advantage of bipolar (electron and hole) nature of transport in inhomogeneously doped semiconductors: a spin-polarized p-n junction^{49,52,53} and a magnetic p-n junction.^{54,57} A spin-polarized p-n junction is a p-n junction with a source spin injected externally into one or both regions (p and n). The source spin can be injected either optically or electrically. We have demonstrated that nonequilibrium spin can be injected (transferred) very effectively across the depletion layer (space-charge region), from both regions: by the majority carriers into the respective minority region, and, vice versa, by the minority carriers into the respective majority region. Spin injection (throughout the paper "spin injection" will mean spin injection through the depletion layer, while externally injected spin will be referred to as "source" spin) by the minority carriers leads to spin accumulation in the majority region, with an effect of amplifying the spin and significantly extending the spin diffusion/drift length.⁵² We have also shown that nonequilibrium spin can be stored and manipulated in a spin-polarized p-n junction by external bias (a spin capacitance effect.⁵² Furthermore, a spin-polarized p-n junction can generate spin-polarized currents as a spin solar cell⁵³ when illuminated by circularly polarized light, a spin-polarized current flows in a p-n junction.

Magnetic p-n junctions⁵⁴ offer even more functionality by coupling equilibrium magnetism and nonequilibrium spin. A magnetic p-n junction is formed by doping a p-n junction with magnetic impurities, differently in the p and n regions. Magnetic impurities induce large g factors of the mobile carriers, thus the application of a magnetic field results in a significant spin splitting of the carrier bands.⁸⁴ If the doping is so large as to induce a ferromagnetic order, the splitting appears also without magnetic field. The important question, of whether spin can be injected by the majority carriers from the magnetic majority region into the nonmagnetic minority one, was answered negative. We have demonstrated that only if nonequilibrium spin is generated first in the majority region, it can subsequently be injected through the depletion layer. Spin can be also injected through the depletion layer at large biases, since then, without any external spin source, nonequilibrium spin is generated by the strong electric field in the bulk regions. We have also shown that magnetoresistance of a magnetic p-n junction increases exponentially with increasing magnetic field (that is, spin band splitting) at large fields. Magnetic p-n junctions exhibit even giant magnetoresistance, when source spin is injected into the majority region. We have also predicted a spin-voltaic effect (the phenomenon related to the Silsbee-Johnson spin-charge coupling^{85,86}) where charge current (or voltage in an open circuit) arises solely due to a nonequilibrium spin maintained in proximity to the magnetic region. Magnetic p-n junctions can also serve as spin valves, since the direction of the zero-bias current can be reversed by reversing either the polarization of the source spin or the direction of the applied magnetic field.

We have studied spin-polarized and magnetic p-n junctions mainly numerically,^{52,53,54} by solving a self-consistent set of recombination-relaxation and drift-diffusion equations, and Poisson's equation. We have obtained solutions

for the carrier and spin densities and currents for small and large biases, and different values of magnetic fields and the externally injected spin polarization. Numerical solution is indispensable at large biases (large injection), where analytical methods are not available. Large bias solutions describe carrier and spin transport as both drift and diffusion, since drift currents due to electric fields are significant even outside of the depletion layer. The low injection regime is tractable analytically. In Ref. 54 we have introduced a heuristic analytical model which accounts well for the numerical findings, and explains all the important qualitative features of magnetic p-n junctions. In fact, our numerical solutions show that the most interesting and potentially important properties of magnetic junctions are at small biases; large biases may still be useful for injecting spin across the depletion layer, or extracting spin from the bulk regions,⁵⁴ as described in Sec. IV E.)

In this paper we formulate a general model of magnetic p-n junctions (the model includes spin-polarized p-n nonmagnetic junctions as a particular case), following the classic formulation of Shockley of ordinary bipolar junctions.^{87,88} The model describes magnetic p-n junctions at small biases (low injection), with arbitrary external (source) spin injection and band spin splitting (magnetic field), within the limits of nondegenerate carrier statistics. The paper has the dual role of describing the fundamental properties of spin-polarized transport in inhomogeneous magnetic semiconductors, while presenting a model simulation, based on the recombination and relaxation limited bipolar drift and diffusion, of novel microelectronics spintronic devices. If semiconductor spintronics is to become a reality, then detailed transport analyses of the type presented in this paper are essential. The fully analytic nature of our theory makes our model simulation particularly useful.

The paper is organized as follows. Section II introduces the model and formulates its assumptions and approximations. Section III describes the spatial profiles of the carrier and spin densities in the bulk regions, gives the boundary conditions for the densities, and discusses the I-V characteristics of magnetic p-n junctions. In Sec. IV we apply our theory to several cases of interest: spin injection (through the depletion layer) by the majority carriers, spin pumping and spin amplification by the minority carriers, source spin injection by the biasing electrode, spin injection and extraction at large biases, and magnetic drift effects in the carrier and spin transport. Finally, we summarize our findings in Sec. V, where we also outline strategies for applying our theory to more realistic materials structures and more complex spintronic devices based on magnetically inhomogeneous semiconductors.

II. MODEL

The basis for our model is a semiconductor p-n junction in which carrier bands are inhomogeneously spin split: there is a finite equilibrium spin polarization of the carriers, different in the p and n regions.⁸⁹ Large (comparable to the thermal energy) spin splitting of carrier bands can arise as a result of doping with magnetic impurities (which may, but need not, contribute to the carrier densities). Magnetic impurities can significantly increase the carrier g factors (usually up to $g \sim 200$ ⁶⁴), so that the application of a magnetic field B induces large spin Zeeman splitting, $2 = g_B B$, of the bands (μ_B is the Bohr magneton). Inhomogeneous spin splitting can be realized either by inhomogeneous magnetic doping in a homogeneous magnetic field, or by a homogeneous magnetic doping in an inhomogeneous magnetic field, or both. Our model applies equally well to ferromagnetic p-n junctions, where bands are spin split even at zero magnetic field. To keep the discussion transparent and to avoid complex notation, we consider only the conduction band to be spin split (that is, only electrons to be spin polarized), keeping holes unpolarized. This simplification does not affect our conclusions, as electron and hole transports are fully separated in our model. (Spin polarization of holes is treated in Appendices A and B.) The layout of a magnetic p-n junction is shown in Fig. 1. The semiconductor is p-doped with N_a acceptors (per unit volume) along the x axis from w_p to 0, and n-doped with N_d donors from 0 to w_n . The depletion layer forms at $(\phi_b; d_n)$. We are not concerned with the transition region itself (we simply assume that it is steep enough (in fact, that it changes over a region smaller than the Debye screening length) to support space charge, and that all the spin splitting changes occur only within the transition region, being constant in both p and n regions (the case of magnetic drift where the splitting is inhomogeneous also in the bulk regions is treated in Sec. IV F)).

We denote the electron density as $n = n(x)$ and the hole density as $p = p(x)$. The corresponding equilibrium values are n_0 and p_0 , and the deviations from the equilibrium values are $n = n_0 + \delta n$ and $p = p_0 + \delta p$. Electron spin density $s = s(x)$ (in equilibrium s_0 and deviation $s = s_0 + \delta s$) is a difference between the densities of spin up and spin down electrons: $s = n_{\uparrow} - n_{\downarrow}$. As a measure of spin polarization we use the spin polarization of the carrier density (not current): $\sigma = s/n$ (in equilibrium σ_0 and deviation $\sigma = \sigma_0 + \delta \sigma$). The equilibrium properties of magnetic p-n junctions are discussed in Appendix A, where n_0 , p_0 , s_0 , and the built-in potential V_b are calculated. The transport parameters of the carriers are diffusivities D_{nn} and D_{np} of electrons in the n and p regions, electron lifetime τ_{np} in the p region, and electron spin lifetime T_{1p} and T_{1n} in the p and n regions. The unpolarized holes are characterized by D_{pn} and τ_{pn} , diffusivity and lifetime in the n region. Throughout the paper, unless explicitly specified otherwise, a single subscript denotes the region or boundary (p, n, L, or R), while a double subscript denotes first the carrier

type or spin (p , n , or s) and then the region or the boundary (for example, τ_{pn} is the lifetime of holes in the n region). Terms "majority" ("minority") will refer to electrons in the n (p) region, and similarly for holes, and not to the more (less) populated spin states, as is usual in the physics of magnetotransport. Similarly, the term bipolar bears no relation to spin, describing only the transport carried by both electrons and holes. Finally, terms "bulk" and, equivalently, "neutral" will denote the regions outside the depletion layer, where, at low biases, charge neutrality is maintained. The notation is summarized in Table I.

The junction is driven out of equilibrium by applying bias and injecting source spin. We place contact electrodes at $x = -w_p$ and $x = w_n$. We keep the left electrode general, capable of injecting electrons, $n_p(-w) \neq 0$, and spin, $s_p(-w) \neq 0$. This boundary condition covers magnetic diodes (ohmic contact, $n_p = 0$), and magnetic solar cells and junction transistors ($n_p \neq 0$). The right electrode is assumed to be ohmic, $p_n(w) = 0$, but able to inject spin, $s_n(w) \neq 0$. The majority carriers in both regions are assumed constant: $p = N_a$ in the p side and $n = N_d$ in the n side. The source spin injection, here considered to take place geometrically at the contacts, can be realized either by the contact electrodes themselves (if the electrodes are magnetic), by optical orientation close to the contact, or by electrical spin injection from a third electrode (say, transverse to the junction current). Different cases mean different boundary conditions for spin. For now we assume a third terminal injection so that s_p and s_n are free parameters of the model; we will later, in Sec. IV D consider the case of the contact (biasing) electrode source spin injection, where s_n will depend on the charge current in the junction.

To reduce the initial drift and diffusion transport problem to a simple diffusion problem in the neutral regions we need to know the boundary conditions for the bulk regions at the depletion layer, that is, the carrier and spin densities $n_L = n(\phi)$, $s_L = s(\phi)$ at the left (L) and $n_R = n(\phi)$, $s_R = s(\phi)$ at the right (R) boundary of the depletion layer. We will calculate these boundary densities in the subsequent sections.

We use several approximations to solve our model. First, we consider only low biases, meaning that the applied forward voltage V is smaller than the built-in field V_b , which is typically about 1 eV. At small biases the densities of the minority carriers are much smaller than the densities of the corresponding majority carriers (the small injection limit), the electric field is confined to the depletion layer, and the bulk regions can be considered neutral. We next assume that the temperature is large enough for the donors and acceptors to be fully ionized, so that $n = N_d$ and $p = N_a$ in the respective majority regions, and the carriers obey the nondegenerate Boltzmann statistics (limiting doping densities to about $10^{18}/\text{cm}^3$ for typical semiconductors at room temperature). Finally, we consider only moderate spin splittings (much smaller than the built-in field), perhaps no greater than $5k_B T$, since greater splittings can severely affect the band structure, and reduce the effective band gap.

We have also made simplifying assumptions as to the band structure of the magnetic semiconductor. First, we neglect possible orbital degeneracy of the bands, and treat the spin states as spin doublets. We also neglect the effects of magnetic doping on the band structure (that is, changes in n_i , additional band sets, etc.) and that of the carrier density on the band spin splitting. The latter can be important in ferromagnetic semiconductors. However, since it is the minority carriers which determine the transport across p - n junctions, it is unlikely that a variation in the carrier density would appreciably affect our conclusions. We also assume that momentum and energy relaxation proceeds much faster than carrier recombination and spin relaxation, so that nonequilibrium, spin-dependent chemical potentials describe well the junction under an applied bias and with a source spin. Finally, we do not consider orbital effects due to the applied magnetic field, although these can be included in our theory simply by allowing for a magnetic dependence of diffusivities.

III. CARRIER AND SPIN TRANSPORT IN THE NEUTRAL REGIONS

The transport of carriers and spin in magnetic p - n junctions can be realistically described as drift and diffusion, limited by carrier recombination and spin relaxation. The transport equations were introduced in Ref. 54, and have been solved numerically for a few important cases in Refs. 52,53,54. Denoting the carrier (here electron) and spin currents as J_n and J_s , the drift-diffusion equations are

$$J_n = D_n (n_t^0 + s^0 - n^0); \quad (1)$$

$$J_s = D_n (s_t^0 + n^0 - s^0); \quad (2)$$

Here ϕ_t is the total local electrostatic potential, comprising both the built-in potential ϕ_b and applied bias V (the electric field is $E = -\phi_t$), and the magnetic drift is proportional to the spatial changes in the band spin splitting, ϕ^0 (see Fig. 1). Throughout this paper we express the potentials and the energies in the units of $k_B T = q$ and $k_B T$, respectively (k_B is the Boltzmann constant, T is the temperature, and q is the proton charge). In a steady state carrier recombination and spin relaxation processes can be expressed through the continuity equations for electrons

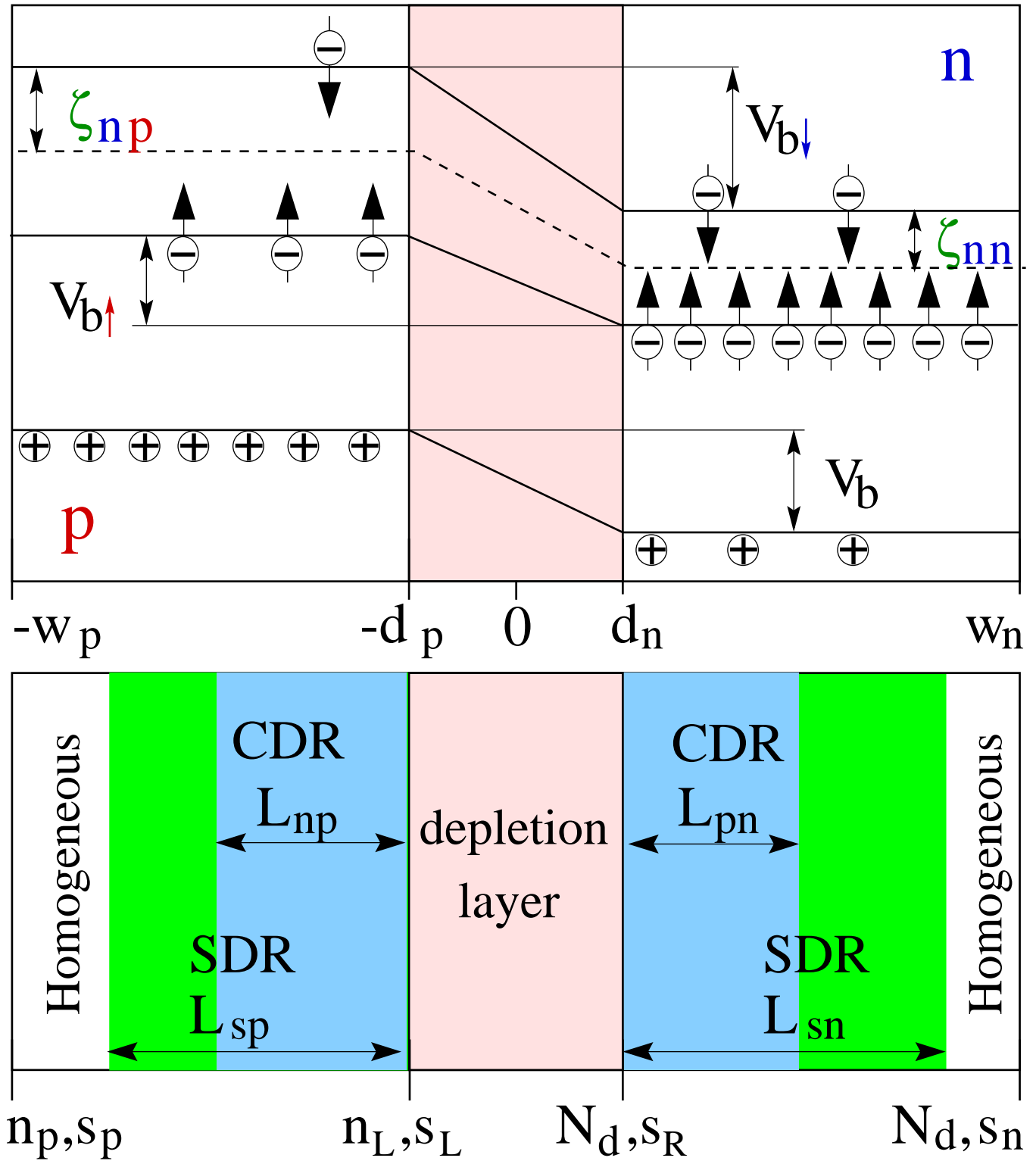


FIG. 1: Schematics of a magnetic p-n junction. The junction is p-doped from $-w_p$ to 0 and n-doped from 0 to w_n . The depletion layer (space-charge region) forms at $-d_p < x < d_n$. The upper figure depicts an inhomogeneously spin-split conduction band and a valence band without the spin splitting. The conduction band spin splitting in the n region is $2\zeta_{nn}$, in the p region it is $2\zeta_{np}$. The greater the ζ , the more is the lower band (here called the spin up sub-band) populated. The intrinsic built-in field across the depletion layer is V_b . For electrons the built-in field becomes explicitly spin dependent: $V_{b*} = V_b + \zeta_{nn} - \zeta_{np}$ and $V_{b\#} = V_b - \zeta_{nn} + \zeta_{np}$. The lower figure depicts regions with distinct transport characteristics: CDR are the (minority) carrier diffusion regions and SDR are the spin (here only electron) diffusion regions. The characteristic sizes of the regions are given by the corresponding diffusion lengths, as indicated. The unshaded areas are the homogeneous regions, where carrier and spin densities assume their equilibrium values. The known (input) densities of the model are n_p, s_p at $-w_p$, and N_d, s_n at w_n , while the densities at the depletion layer, n_L and s_L on the left side and $n_R = N_d, s_R$ on the right side, are calculated in the text.

N_d	=	donor density
N_a	=	acceptor density
n	=	electron density (equilibrium n_0)
p	=	hole density (p_0)
s	=	spin density (s_0)
$s = n$	=	spin polarization (s_0)
$s = s_0 n$	=	effective nonequilibrium spin density
J_n	=	electron particle current
j_n	=	qJ_n , electron charge current
J_p	=	hole particle current
j_p	=	qJ_p , hole charge current
J_s	=	spin current
n_p	=	electron density at $x = -w_p$ (n_{0p})
n_L	=	electron density at $x = -d_p$ ($n_{0L} = n_{0p}$)
s_p	=	spin density at $x = -w_p$ (s_{0p})
s_n	=	spin density at $x = w_n$ (s_{0n})
s_L	=	spin density at $x = -d_p$ ($s_{0L} = s_{0p}$)
s_R	=	spin density at $x = d_n$ ($s_{0R} = s_{0n}$)
w_p	=	$w_p - d_p$, effective width of the p region
w_n	=	$w_n - d_n$, effective width of the n region
D_{nn}	=	electron diffusivity in the n region
D_{np}	=	electron diffusivity in the p region
τ_{np}	=	lifetime of electrons in the p region
τ_{pn}	=	lifetime of holes in the n region
L_{np}	=	$\sqrt{D_{np} \tau_{np}}$, electron diffusion length in the p region
L_{pn}	=	$\sqrt{D_{pn} \tau_{pn}}$, hole diffusion length in the n region
T_{1p}	=	intrinsic spin lifetime in the p region
L_{1p}	=	$\sqrt{D_{np} T_{1p}}$, intrinsic spin decay length in the p region
$1/\tau_{sp}$	=	$1/\tau_{np} + 1/T_{1p}$, spin decay rate in the p region
L_{sp}	=	$\sqrt{D_{np} \tau_{sp}}$, spin diffusion length in the p region
T_{1n}	=	spin lifetime in the n region
L_{sn}	=	$\sqrt{D_{nn} T_{1n}}$, spin diffusion length in the n region
V_b	=	built-in potential
V	=	applied bias

TABLE I: Summary of the notation used in the text and in Table II. All the spin parameters (spin density, spin lifetime, etc.) relate to electrons. In the brackets are the equilibrium densities.

and spin:

$$J_n^0 = -r(np - np_0); \quad (3)$$

$$J_s^0 = -r(sp - sp_0) - \frac{s}{T_1}; \quad (4)$$

where r is the electron-hole recombination rate and $s = s_0 n$, expressing the fact that intrinsic spin relaxation processes (spin- $\uparrow\downarrow$ scattering, say, by phonons or impurities) conserve the local carrier density.^{4,54} Electron-hole recombination also degrades spin, the fact reflected in the first term of Eq. (4). Equations (1), (2), (3), and (4), together with Poisson's equation $\nabla \cdot \mathbf{E} = \rho/\epsilon$ ($\rho = qN$), where ρ is the local charge density and ϵ is the semiconductor's dielectric constant, fully describe the steady-state carrier and spin transport in inhomogeneous magnetic semiconductors.⁵⁴ In the rest of the paper (except for Sec. IV F), magnetic drift force will play no explicit role, since we assume that the magnetic doping is uniform in the bulk regions. The inhomogeneity in the spin splitting, which is confined to the depletion region, will appear only through the boundary conditions.

At low biases, the case most important for device applications, the problem of the carrier and spin transport in magnetic p-n junctions reduces to the problem of carrier and spin diffusion in the neutral regions.^{87,88} This observation,

to be useful, needs to be furnished with the boundary conditions for the carrier and spin densities at the depletion layer boundary (n_L , s_L , n_R , and s_R). Shockley's model⁸⁷ evaluates the carrier densities in unpolarized p-n junctions from the assumption that a quasiequilibrium is maintained in the depletion layer even at applied (low) biases. This assumption alone is insufficient to obtain both carrier and spin densities in a spin-polarized magnetic junction. We use, in addition, the continuity of the spin current in the depletion layer to calculate the densities. A simple version of this model was introduced in Ref. 54, where it was assumed that (1) at a forward bias and with a source spin injected into the majority region ($s_L \neq 0$) the spin current at the depletion layer, J_{sR} , vanishes, and (2) at a reverse bias, and with spin injected into the minority region ($s_R \neq 0$), all the spin entering the depletion region is swept by the large built-in field to the majority side. Assumption (1) explains spin injection of nonequilibrium spin through the depletion layer, while (2) explains spin pumping by the minority carriers. Both assumptions will follow as special cases of the spin current continuity, in our model.

In analogy with unpolarized p-n junctions,⁹⁰ there are several regions with distinct transport characteristics in spin-polarized magnetic p-n junctions, as illustrated in Fig. 1: (i) the depletion layer with space charge and large carrier and spin drift and diffusion; (ii) the carrier diffusion regions (CDR) which are neutral and where the minority carriers' drift can be neglected. CDR are characterized by carrier diffusion lengths L_{np} for electrons on the p side and L_{pn} for holes on the n side; (iii) the spin diffusion regions (SDR), which are neutral and where spin (both majority and minority) drift can be neglected. SDR are characterized by spin diffusion length L_{sp} on the p side and L_{sn} on the n side; (iv) the homogeneous regions in the rest of the junction, which are neutral, and where the carrier and spin densities assume their equilibrium values. There is no diffusion, only the majority carriers' drift.

This section presents a unified picture of carrier and spin transport in magnetic p-n junctions. We first describe the profiles of carrier and spin densities inside the bulk regions, as dependent on the densities at the depletion layer, which are calculated next by modifying Shockley's model to the spin polarized case. The four (not independent) important assumptions used are (a) neutrality of the bulk regions, (b) small injection of the carriers across the depletion layer and at the biasing contacts, (c) the existence of a thermal quasi-equilibrium across the depletion layer even under applied bias and source spin, and (d) continuity of spin current across the depletion layer. Our analytical results, summarized in Table II, show how the carrier density is influenced by both bias (as in the unpolarized case) and nonequilibrium spin, and, vice versa, how nonequilibrium spin is influenced by both bias and nonequilibrium carrier density. This interplay is imprinted most significantly in the dependence of the I-V characteristics of the magnetic diodes on nonequilibrium spin.

A. Carrier and spin profiles

1. p region

In the p region the hole density is uniform, $p = N_a$. Electrons are the minority carriers whose diffusion is governed by the equation

$$n'' = \frac{n}{L_{np}^2}; \quad (5)$$

where the electron diffusion length is $L_{np} = \sqrt{D_{np} \tau_{np}}$. We remind that if two subscripts are used in a label, the first denotes the carrier type (p or n) or spin (s), and the second the region or the boundary (p, n, L, or R); if only one subscript is used, it denotes the region or the boundary. Equation (5) is obtained by combining Eqs. (1) and (3), neglecting the electric drift force (magnetic drift vanishes in the bulk regions), and defining $l = \tau_{np} / N_a$. The boundary conditions for the electron density are n_p at $x = -w_p$ and n_L (yet unknown) at $x = -\phi_p$. The boundary position of the depletion layer is not fixed, but changes with the applied voltage and the equilibrium magnetization (through V_b , see Appendix A) as

$$\phi_p = \frac{s}{q} \frac{2 N_d V_b - V}{N_a N_a + N_d}; \quad (6)$$

It is useful to introduce $w_p = w_p - \phi_p$ to describe the effective width of the p region. The solution of Eq. (5) can then be written as

$$n = n_L \cosh(x_{np}) + F_{np} \sinh(x_{np}); \quad (7)$$

where $x_{np} = (x + \phi_p)/L_{np}$ and

$$F_{np} = \frac{n_L \cosh(w_p/L_{np}) - n_p}{\sinh(w_p/L_{np})}; \quad (8)$$

"Flux" parameters F are central to our analysis, since they determine the currents at the depletion layer. Effectively, F measures the change in the nonequilibrium (here carrier n) density over the length scales of the (here carrier L_{np}) diffusion length: For a short p region, $L_{np} \ll w_p$, $F_{np} = (n_L - n_0)/L_{np} = w_p$, while for $L_{np} \gg w_p$, $F_{np} = n_L$. The electron current profile, $J_n = -D_{np} \nabla n$, is

$$J_n = -\frac{D_{np}}{L_{np}} [n_L \sinh(x/L_{np}) + F_{np} \cosh(x/L_{np})] \quad (9)$$

At the depletion layer, $x = 0$, the current is

$$J_{nL} = -\frac{D_{np}}{L_{np}} F_{np} \quad (10)$$

The spin density is also described by a diffusion equation. From Eqs. (2) and (4), under the conditions of charge neutrality and magnetic uniformity, we obtain

$$s'' = \frac{s}{L_{sp}^2} - \frac{1}{L_{sp}^2} \frac{n}{n_0} \quad (11)$$

where $L_{1p} = \sqrt{D_{np}/T_{1p}}$ and the effective spin diffusion length in the p region is $L_{sp} = \sqrt{D_{np}/\Gamma_{sp}}$, where $\Gamma_{sp} = \Gamma_{np} + \Gamma_{1p}$ is the effective spin relaxation rate, reflecting the fact that, in addition to intrinsic spin relaxation processes, carrier recombination degrades spin. The second term in the RHS of Eq. (11) acts as a local spin source, and appears because a change in the electron density, n , drives spin by intrinsic spin relaxation processes to n_0 [see Eq. (4)], thereby preserving the equilibrium spin polarization, but not the spin itself. The boundary conditions for the spin density are $s_p = s(0)$ and, yet unknown, $s_L = s(L)$. The solution of Eq. (11) is

$$s = s_p \cosh(x/L_{sp}) + F_{sp} \sinh(x/L_{sp}) + n_0 \quad (12)$$

where $s_p = s(0)$, $s_L = s(L)$, and n_L is the effective nonequilibrium spin at L , and

$$F_{sp} = \frac{s_L \cosh(w_p/L_{sp}) - s_p}{\sinh(w_p/L_{sp})} \quad (13)$$

is a normalized spin flux with $s_p = s_p - n_0$. For a large spin diffusion length, $L_{sp} \gg w_p$, $F_{sp} = (s_L - s_p)/L_{sp} = w_p$, while for $L_{sp} \ll w_p$, $F_{sp} = s_L$. The first two terms in the RHS of Eq. (12) describe the deviation of the spin density from n_0 , while the last term represents the deviation $n - n_0$ which is solely due to intrinsic spin relaxation (T_1) processes. The spin current, $J_s = -D_{np} \nabla s$, has the profile

$$J_s = -\frac{D_{np}}{L_{sp}} [s_L \sinh(x/L_{sp}) + F_{sp} \cosh(x/L_{sp})] + n_0 J_n \quad (14)$$

The first two contributions describe the spin flow due to spatial variations in s , while the last term represents the spin flow associated with the spin-polarized electron current. Finally, at the depletion layer, $x = 0$, the spin current is

$$J_{sL} = -\frac{D_{np}}{L_{sp}} F_{sp} + n_0 J_{nL} \quad (15)$$

The first term can be neglected if the spin polarization is close to its equilibrium value (which is typically the case at small biases and no source spin). The second term is important for spin extraction at large biases (see Sec. IV E).

2. n region

In the n region only spin diffusion needs to be examined, as to a very good approximation $n = N_d$ (charge neutrality actually requires that $n = N_d + p$, where p is the deviation of the hole density from equilibrium; this gives a small contribution to spin density s_h , as is discussed in Sec. IV E and Appendix C). Electron spin diffusion is described by the equation (obtained from Eqs. (2) and (4) neglecting electric and magnetic drifts and recombination processes, as $p \ll N_d$)

$$s'' = \frac{s}{L_{sn}^2} \quad (16)$$

where $L_{sn} = \frac{D_{nn}}{T_{1n}}$. We introduce $w_n = w_n - d_n$ as the effective width of the neutral region, with bias and equilibrium spin polarization dependent depletion layer boundary

$$d_n = \frac{s}{q} \frac{N_a V_b - V}{N_d N_a + N_d} : \quad (17)$$

The boundary conditions for the spin density are $s_R = s(w_n)$ and $s_n = s(d_n)$. The solution of Eq. (16) is

$$s = s_R \cosh(w_n) + F_{sn} \sinh(w_n); \quad (18)$$

where $w_n(x - d_n) = L_{sn}$ and

$$F_{sn} = \frac{s_n - s_R \cosh(w_n = L_{sn})}{\sinh(w_n = L_{sn})} : \quad (19)$$

The normalized flux is $F_{sn} = (s_n - s_R) L_{sn} = w_n$ for a short n region, $L_{sn} = w_n$, while $F_{sn} = s_R$ when $L_{sn} = w_n$. The spin current, $J_s = D_{nn} \frac{ds}{dx}$, is

$$J_s = \frac{D_{nn}}{L_{sn}} [s_R \sinh(w_n) + F_{sn} \cosh(w_n)] : \quad (20)$$

Finally, at the depletion layer, $x = d_n$, the spin current is

$$J_{sR} = \frac{D_{nn}}{L_{sn}} F_{sn} : \quad (21)$$

The spin current at the depletion layer boundary is solely the diffusion current due to a spatially inhomogeneous nonequilibrium spin in the region. Electrons with just the equilibrium spin polarization will not contribute to spin flow within the model approximations (see Sec. IV E for a discussion of how the neglected terms affect the carrier and spin transport).

B. Carrier and spin densities at the depletion layer

Let $\phi(x)$ be the electrostatic potential resulting from the application of applied bias V (that is, not including the equilibrium built-in potential V_b). We assume that all the applied bias drops within the high resistance, carrier devoid, depletion layer:

$$\phi(d_n) - \phi(d_n) = V; \quad (22)$$

so that ϕ is constant in the bulk regions. Further, let μ be the deviation of the nonequilibrium chemical potential from its equilibrium value; μ is generally spin dependent: we will denote it as μ_{\uparrow} for spin up and μ_{\downarrow} for spin down electrons. That μ is a good description of the carrier and spin nonequilibrium energy distribution follows from the well established fact that energy and momentum relaxation proceeds much faster than carrier recombination and spin relaxation. For a nondegenerate statistics, spin up and spin down electron densities can be written as

$$n_{\uparrow}(x) = n_{\uparrow 0}(x) \exp[\phi(x) + \mu_{\uparrow}(x)]; \quad (23)$$

$$n_{\downarrow}(x) = n_{\downarrow 0}(x) \exp[\phi(x) + \mu_{\downarrow}(x)]; \quad (24)$$

where $n_{\uparrow 0}$ and $n_{\downarrow 0}$ are the equilibrium values; we have made explicit the fact that all the quantities describing the densities vary in space. The electron, $n = n_{\uparrow} + n_{\downarrow}$, and spin, $s = n_{\uparrow} - n_{\downarrow}$, densities are

$$n = \exp(\phi + \mu) [n_0 \cosh(\mu) + s_0 \sinh(\mu)]; \quad (25)$$

$$s = \exp(\phi + \mu) [n_0 \sinh(\mu) + s_0 \cosh(\mu)]; \quad (26)$$

where $\mu = (\mu_{\uparrow} - \mu_{\downarrow})/2$. Finally, the spin polarization

$$P = \frac{\tanh(\mu) + \mu_0}{1 + \mu_0 \tanh(\mu)} \quad (27)$$

depends on μ only (while n and s depend on both ϕ and μ).

Substituting Eqs. (25) and (26) into the equations (1) and (2) for the electron carrier and spin currents, we obtain,

$$J_n = D_n \nabla_x n_+^0 + s_+^0 ; \quad (28)$$

$$J_s = D_n \nabla_x n_+^0 + s_+^0 : \quad (29)$$

It may be tempting to associate s_+ with only charge, and s_- with only spin (as done, for example, in Ref. 91). It would then follow from Eq. (28) that in a semiconductor with a uniform carrier density a charge current would flow (or a spin emf would appear) if a nonequilibrium spin gradient (or, equivalently here, spin polarization gradient) would be maintained.⁹¹ This is wrong, as can be seen directly from Eq. (1) which shows that spin can contribute to charge current only through magnetic drift (see Sec. IV F), $\nabla_x s_+^0$. Although s_+^0 indeed succeeds to determine J_n , it also influences n_+ . If n_+ is to be uniform and s_+ has a finite gradient, then s_+ must change to ensure that n_+ is unchanged, as follows from Eq. (25). However, a spin emf due to spin polarization gradient would appear in degenerate semiconductors or metals,⁹¹ as mobilities and diffusivities for spin up and down species would generally be different in this case, and spin diffusion directly affects charge current.⁵⁴

1. Shockley's condition of constant chemical potentials

We now apply the condition of constant chemical potentials in the depletion layer to connect the charge and spin densities at the left (L) and right (R) depletion layer edges. First notice that

$$\tanh(\phi) = \frac{s_+^0(x) - s_-^0(x)}{1 - s_+^0(x)s_-^0(x)} = \text{const}; \quad (30)$$

from which follows that the spin polarizations at L and R are connected without an explicit dependence on bias. We will now express n_L , n_R , and s_L in terms of the nonequilibrium spin polarization in the n region, $s_R = s_R - N_d$; we will evaluate s_R explicitly from the input parameters in the next section.

It follows from Eq. (30) that

$$s_L = \frac{s_{0L}(1 - s_{0R}^2) + s_R(1 - s_{0L}s_{0R})}{1 - s_{0R}^2 + s_R(s_{0L} - s_{0R})}; \quad (31)$$

If $s_R = 0$, then $s_L = s_{0L}$. In other words, only nonequilibrium spin can be injected from the majority region through the depletion layer. In the case of a homogeneous spin splitting ($s_{0L} = s_{0R}$), $s_L = s_R$, that is, the nonequilibrium spin polarization is constant across the depletion layer. Also note that s_L depends on the applied bias only implicitly, through the possible bias dependence of s_R .

The carrier and spin densities at L are determined by both s_R and V . Equations (25) and (26) yield

$$n_L = n_{0L} e^V \left[1 + s_R \frac{s_{0L} - s_{0R}}{1 - s_{0R}^2} \right]; \quad (32)$$

$$s_L = s_{0L} e^V \left[1 + \frac{s_R}{s_{0L}} \frac{1 - s_{0L}s_{0R}}{1 - s_{0R}^2} \right]; \quad (33)$$

In the absence of nonequilibrium spin ($s_R = 0$), the above formulas reduce to the well known Shockley relation for the minority carrier density at the depletion layer,⁸⁷ $n_L = n_{0L} \exp(V)$, and the analogous formula for spin, $s_L = s_{0L} \exp(V)$, so that the equilibrium spin polarization $s_L = s_{0L}$ is preserved. Equations (32) and (33) demonstrate the interplay between charge and spin in magnetic p-n junctions: nonequilibrium spin s_R can significantly affect the minority carrier density (thus the junction I-V characteristics, as will be shown in Sec. III C) and spin, while bias affects both the carrier and spin densities. If the band spin splitting is homogeneous ($s_{0L} = s_{0R}$), nonequilibrium spin does not influence the minority carrier density [and affects the spin density in a trivial way: $s_L = n_{0L} s_L \exp(V)$]. Equation (32) suggests that the charge response, n_L , to nonequilibrium spin can be maximized by maximizing the difference in the equilibrium spin polarizations, $|s_{0L} - s_{0R}|$, and having s_{0R} as close to 1 as possible (the case of $s_{0R} = 1$ is pathological, and is excluded from our theory by the assumption of small injection, whereby $n_L \ll N_a; N_d$).

2. Continuity of spin current in the depletion layer

In the previous sections s_R was treated as an unknown input parameter to obtain the carrier and spin profiles, and specially the carrier and spin densities at $x = x_d$. Calculation of s_R is performed in this section. The

knowledge of μ_R will complete the formalism necessary to calculate any quantity of the magnetic p-n junction under general conditions of applied bias and source spin, with the stated constraints of the model. In the spin-equilibrium case ($\mu = 0$) the calculation made in the preceding section suffices to get all the necessary boundary conditions. The reason is that the carrier density in the majority side is uniform, $n = N_d$. Spin, however, does not behave similarly to the majority carriers even in the majority region. Spin can be injected into the majority region, and diffuses, rather than drifts, there. This is why the unknown μ_R needs to be specified by another condition. Here we apply the condition of the continuity of spin current in the depletion layer. Physical justification for this condition is the fact that in the depletion layer, devoid of carriers and spin, spin relaxation, proportional to the spin density, is inhibited. One can write from Eq. (4)

$$J_{sR} = J_{sL} - J_{s,relax}; \quad (34)$$

where $J_{s,relax}$ is the spin relaxation current (similar to the carrier recombination current used in treating unpolarized junctions⁸⁸),

$$J_{s,relax} = \int_{d_p}^{Z_{dn}} dx \left(r(sp - sp_0) + \frac{s}{T_1} s \right); \quad (35)$$

We neglect $J_{s,relax}$ in the following treatment.⁹²

Equations (15), (21), (32), and (33), together with Eq. (34), form a full, self-consistent set of equations needed to extract q_R (or, equivalently, μ_R), and thus complete the structure of the model. In the process of extracting q_R , we apply the condition of low injection, and neglect the terms of the order of $n_{0L} \exp(V)$ when compared to N_d . The result is

$$q_R = q_0 s_n + q_1 sp + q_2 n_{0L} n_p - q_3 s_{0L} e^V - 1; \quad (36)$$

where the geometric/transport factors are

$$q_0 = 1 = \cosh(w_n = L_{sn}); \quad (37)$$

$$q_1 = \frac{D_{np}}{D_{nn}} \frac{L_{sn}}{L_{sp}} \frac{\tanh(w_n = L_{sn})}{\sinh(w_p = L_{sp})}; \quad (38)$$

$$q_2 = \frac{D_{np}}{D_{nn}} \frac{L_{sn}}{L_{np}} \frac{\tanh(w_n = L_{sn})}{\sinh(w_p = L_{np})}; \quad (39)$$

$$q_3 = q_2 \cosh(w_p = L_{np}); \quad (40)$$

Equation (36) expresses q_R in terms of the known input parameters, and can be used as an input for determining the carrier and spin densities at the depletion layer, as well as the carrier and spin profiles in the bulk regions. The first contribution to q_R comes from the source spin at the right contact, s_n . The second and the third terms in the RHS of Eq. (36) come from the source spin and the carrier densities at the left contact, and a result of spin injection by the minority electrons through the depletion layer. Finally, the last term, which usually is negligible, results from the spin flow of the minority electrons having the equilibrium spin polarization (that is, as if no spin or minority electron source were present). This term, for large forward biases, leads to spin extraction (see Sec. IV E). In most practical cases the source spin is injected either in the majority or in the minority regions, not both. Then the contributions to q_R can be considered separately, with either the first, or the second and the third terms in the RHS of Eq. 36 contributing. The last term (that with q_3) can be usually neglected in the low injection limit. Implications of Eq. (36) for spin-polarized transport in magnetic p-n junctions will be explored in Sec. IV.

The content of this and the previous sections is summarized in Table II.

C. I-V characteristics

Charge current in a magnetic p-n junction is driven by both external bias and source spin. Neglecting carrier recombination in the depletion layer, the charge electron current is the current that appears at the depletion layer in the minority side, $x = \phi$: $j_h = qJ_{hL}$. Equation (10) gives

$$j_h = j_{0n} + j_{1n} + j_{2n}; \quad (41)$$

p region carrier density and current	
$n^0 = n = L_{np}^2$	
$n = n_L \cosh(w_p) + F_{np} \sinh(w_p)$	
$J_n = D_{np} n^0$	
$J_n = (D_{np} = L_{np}) [n_L \sinh(w_p) + F_{np} \cosh(w_p)]$	
n_p	$(x + d_p) = L_{np}$
F_{np}	$[n_L \cosh(w_p = L_{np}) - n_p] = \sinh(w_p = L_{np})$
n_L	$n_{0L} e^V \left(1 + \frac{R}{R} \left(\frac{0L}{0L} - \frac{0R}{0R} \right) \right) = (1 - \frac{2}{0R}) n_{0L}$
J_{nL}	$(D_{np} = L_{np}) F_{np}$
p region spin density and current	
$s^0 = s = L_{np}^2 + s = L_{lp}^2$	
$s = s_L \cosh(w_p) + F_{sp} \sinh(w_p) + s_{0p} n$	
$J_s = D_{np} s^0$	
$J_s = (D_{np} = L_{sp}) [s_L \sinh(w_p) + F_{sp} \cosh(w_p)] + s_{0p} J_n$	
s_p	$(x + d_p) = L_{sp}$
s_L	$s_L - s_{0L} n_L$
s_p	$s_p - s_{0p} n_p$
F_{sp}	$[s_L \cosh(w_p = L_{sp}) - s_p] = \sinh(w_p = L_{sp})$
s_L	$s_{0L} e^V \left(1 + \left(\frac{R}{R} = \frac{0L}{0L} \right) \left(1 - \frac{0L}{0L} - \frac{0R}{0R} \right) \right) = (1 - \frac{2}{0R}) s_{0L}$
J_{sL}	$(D_{np} = L_{sp}) F_{sp} + s_{0L} J_{nL}$
n region spin density and current	
$s^0 = s = L_{sn}^2$	
$s = s_R \cosh(w_n) + F_{sn} \sinh(w_n)$	
$J_s = D_{nn} s^0$	
$J_s = (D_{nn} = L_{sn}) [s_R \sinh(w_n) + F_{sn} \cosh(w_n)]$	
s_n	$(x - d_n) = L_{sn}$
F_{sn}	$[s_n - s_R \cosh(w_n = L_{sn})] = \sinh(w_n = L_{sn})$
s_R	$s_{0n} s_n + s_{1p} s_p + s_{20L} n_p + s_{30L} e^V - 1$
0	$1 = \cosh(w_n = L_{sn})$
1	$(D_{np} = D_{nn}) (L_{sn} = L_{sp}) [\tanh(w_n = L_{sn}) = \sinh(w_p = L_{sp})]$
2	$(D_{np} = D_{nn}) (L_{sn} = L_{np}) [\tanh(w_n = L_{sn}) = \sinh(w_p = L_{np})]$
3	$s_{20L} \cosh(w_p = L_{np})$
J_{sR}	$(D_{nn} = L_{sn}) F_{sn}$

TABLE II: The carrier and spin densities and currents in the bulk regions of a magnetic p-n junction. Only electrons are spin polarized (spin polarization of holes is treated in Appendices A and B). For both the p and n regions, the diffusion equations and the equations for currents, as well as the explicit formulas describing the spatial profiles of the densities and currents in the bulk regions are given. The notation is summarized in Table I.

where

$$j_{0n} = j_{gn} e^V - 1; \quad (42)$$

$$j_{1n} = j_{gn} e^V \left(\frac{0L}{1} - \frac{0R}{2} \right); \quad (43)$$

$$j_{2n} = j_{gn} \frac{1}{\cosh(w_p = L_{np})} \frac{n_p}{n_{0L}}; \quad (44)$$

By j_{gn} we denote the electron generation current (current of thermally excited electrons in the p region close to the depletion layer⁸⁸):

$$j_{gn} = \frac{q D_{np}}{L_{np}} n_{0L} \coth \frac{w_p}{L_{np}}; \quad (45)$$

The generation current depends on the equilibrium magnetization through n_{0L} (see Appendix A). A magnetic p-n junction works as a diode when both electrodes are Ohmic ($n_p = 0$), in which case $j_h = j_{0n} + j_{1n}$. This current can be also written as

$$j_{0n} + j_{1n} = j_{gn} \frac{n_L}{n_{0L}}; \quad (46)$$

a notation which emphasizes the crucial role of the minority carrier density at the depletion layer for charge transport. Equation (42) describes the usual rectification current, which (for an Ohmic contact) is the only carrier current in magnetically homogeneous junctions ($n_{0L} = n_{0R}$), or in junctions lacking nonequilibrium spin ($j_R = 0$). Once a nonequilibrium spin is present, and the carrier bands are inhomogeneously spin split, the current is modified by j_{1n} , the spin-voltaic current, the charge current caused by nonequilibrium spin. The spin-voltaic current does not vanish at zero bias, giving rise to the spin-voltaic and spin-valve effects⁵⁴ discussed in Sec. IV C. Including the hole current (see Appendix B), the total charge current reads

$$j = j_n + j_p; \quad (47)$$

Here we consider holes to be unpolarized, so that

$$j_p = j_{gp} (e^V - 1); \quad (48)$$

with

$$j_{gp} = \frac{qD_{pn}}{L_{pn}} p_{0R} \coth(\kappa_n = L_{pn}) \quad (49)$$

being the hole generation current. The hole current is affected by magnetic field only through p_{0R} (see Appendix A). If also holes would be spin polarized, the hole current would depend on the nonequilibrium hole spin polarization, and would exhibit all the spin phenomena we discuss for electrons. The corresponding formulas are presented in Appendix B.

For spin injection problems it is often useful to consider the spin polarization of the charge current, not only the density spin polarization. The current spin polarization is defined as $j_J = j_s/j$, where j_s is the spin current associated with charge flow. In our case of only electrons being spin polarized, $j_s = qI_s$. Since j is a conserved quantity, the spin polarization profile is the same as the profile of the spin current, already given in the previous sections. As will also be demonstrated in the discussion of particular cases of interest, j_J can differ significantly from 1. Unlike for j_s , for example, the magnitude of j_J can be greater (even much greater) than unity (if spin up and down electrons flow in opposite directions). The knowledge of the current spin polarization is essential particularly in studies of spin injection, where typically one assumes that j_J is conserved across the injection interface (see Sec. IV D), as a result of the continuity of the spin current.

We close this section by explaining qualitatively the physics behind the spin-voltaic current j_{1n} . Equation (41) can be understood rather simply by considering the balance between the recombination and generation currents in the depletion layer.⁹⁰ In the following we put $n_p = 0$, to simplify the discussion. Let n_n and n_p denote the conduction band splitting in the n and p regions, respectively, as illustrated in Fig. 1. The recombination electron current is the current of the majority electrons flowing from n to p. It is essentially the current of electrons with enough energy to cross the potential barrier in the depletion layer. This barrier is different for spin up ($V_{b\#} = V_b + n_n - n_p$) and spin down ($V_{b\#} = V_b - n_n + n_p$) electrons. Within the Boltzmann statistics the recombination current of spin up and down electrons, under applied bias V , is

$$j_{r\#} = K n_R n_{\#} e^{V_{b\#} - n_n + n_p + V}; \quad (50)$$

$$j_{r\#} = K n_R n_{\#} e^{V_{b\#} - n_n - n_p + V}; \quad (51)$$

where K is a spin-independent constant. The recombination current is proportional to the number of electrons n_R available for thermal activation over the barrier, and the thermal activation Boltzmann factor $\exp(-V_b + V)$.

The generation currents are the electron currents (flowing from p to n) due to the minority electrons thermally generated in the diffusion region on the p side (Fig. 1), and swept by the large built-in field to the n side. The generation currents are bias independent, and must equal the corresponding recombination currents if $V = 0$, so that no net current flows in equilibrium. Thus

$$j_g = K n_{0R} n_{\#} e^{V_{b\#} - n_n + n_p}; \quad (52)$$

$$j_g = K n_{0R} n_{\#} e^{V_{b\#} - n_n - n_p}; \quad (53)$$

The total electron charge current, $j_n = j_n^{\text{ex}} + j_n^{\text{in}} + j_n^{\text{re}} + j_n^{\text{dr}}$, can be expressed through the equilibrium and nonequilibrium electron spin polarizations, using formulas from Appendix A. The result is

$$j_n = K n_{0L} e^V \left(1 + \frac{\phi_L}{1} \frac{\phi_R}{2} \right) \quad (54)$$

which is, up to a constant, Eq. (41) (the constant K , which is proportional to the generation current, can be obtained rigorously only by solving the corresponding diffusion equations). The above reasoning explains the spin-voltaic effect in magnetic p-n junctions as resulting from the disturbances of the balance between the generation and recombination currents. The nonequilibrium spin itself, ϕ_R , which is an input for Eq. (43), must be obtained by considering the full set of assumptions leading to Eq. (36).

IV. DISCUSSION

As an application of our theory we discuss several important manifestations of spin-polarized bipolar transport in magnetic p-n junctions, and illustrate the examples numerically with GaAs materials parameters. The specific cases we consider are spin injection (through the depletion layer) by the majority carriers, spin pumping by the minority carriers, the spin-voltaic effect, external (source) spin injection by the biasing electrode, spin injection and extraction at large biases, and magnetic drift in the neutral regions.

The reason for choosing GaAs for numerical examples is that GaAs is the best studied semiconductor for spin properties.⁴ Spin can be injected into GaAs both optically and electrically, and high quality magnetic hybrid semiconductor structures based on GaAs can be potentially fabricated, as underlined by the discovery of ferromagnetic (Ga,Mn)As.^{31,32} For integration with semiconductor technology, however, it would be much more desirable to have Si-based spintronic devices. Although optical orientation⁴ of electron spins in Si is not effective because of the band structure (unlike GaAs, Si is not a direct band-gap semiconductor), there seems to be no fundamental reason why spin could not be injected into Si electrically; thus far, however, electrical spin injection into Si has proved elusive.⁹³ In addition to the economic reasons of easy technological integration, Si could offer other advantages over GaAs, such as (expected) longer spin relaxation times (due to the weak spin-orbit coupling and the absence of the D'yakonov-Perel' mechanism^{4,18} of spin relaxation in centrally symmetric Si), and much larger intrinsic carrier density n_i (important for bipolar conduction).

The numerical examples in the following sections are all based on a symmetric GaAs magnetic diode with the fixed parameters $N_a = N_d = 10^{16} \text{ cm}^{-3}$, $n_i = 1.8 \cdot 10^6 \text{ cm}^{-3}$, $D_n = 100 \text{ cm}^2/\text{s}$, and $\tau_n = \tau_p = 1 \text{ ns}$ (equal in both regions), $w_p = w_n = 3 \text{ }\mu\text{m}$. The derived parameters are $L_{np} = 32 \text{ }\mu\text{m}$, $L_{sp} = 22 \text{ }\mu\text{m}$, and $L_{sn} = 32 \text{ }\mu\text{m}$. Other parameters (bias, equilibrium and nonequilibrium spin) will be specified according to the physical situation. The materials parameters are for room temperature, so the chemical potentials will be given in the units of $k_B T = 25 \text{ meV}$.

A. Spin injection by the majority carriers

Under the low injection conditions nonequilibrium spin cannot build up in magnetic p-n junctions, as was shown in Secs. IIIB 1 and IIIB 2. Only if a nonequilibrium (source) spin is externally injected into either region of the junction, spin injection through the depletion layer is possible. Here we consider the case with a magnetic n side ($\phi_R \neq 0$) and a nonmagnetic p side ($\phi_L = 0$), and inject the source spin at the right contact (but not by the contact itself), so that $\phi_n \neq 0$. The left contact remains Ohmic with equilibrium carriers and spin ($\phi_p = \phi_s = 0$). The nonequilibrium spin at the depletion layer in the n region is obtained from Eq. (36) (see also Table II) as

$$\phi_n = \phi_R N_d = \frac{S_n}{\cosh(w_n/L_{sn})} \quad (55)$$

This boundary condition for spin at the depletion layer can be physically formulated by requiring that the spin current of the majority carriers vanishes at the depletion layer.⁵⁴ This is quite natural to assume, since the spin current in the n side is proportional to $\phi_n N_d$, while the spin current in the p side is proportional to the much smaller $\phi_p N_a$. Since $J_{SR} = J_{SL}$, we can neglect J_{SR} relative to J_s in the rest of the n region. Eq. (55) then follows.

On the left side of the depletion layer the Shockley condition, according to Eqs. (32) and (33), gives for the electron and spin densities

$$n_L = n_{0L} e^V \left(1 + \frac{\phi_R}{1} \frac{\phi_R}{2} \right) \quad (56)$$

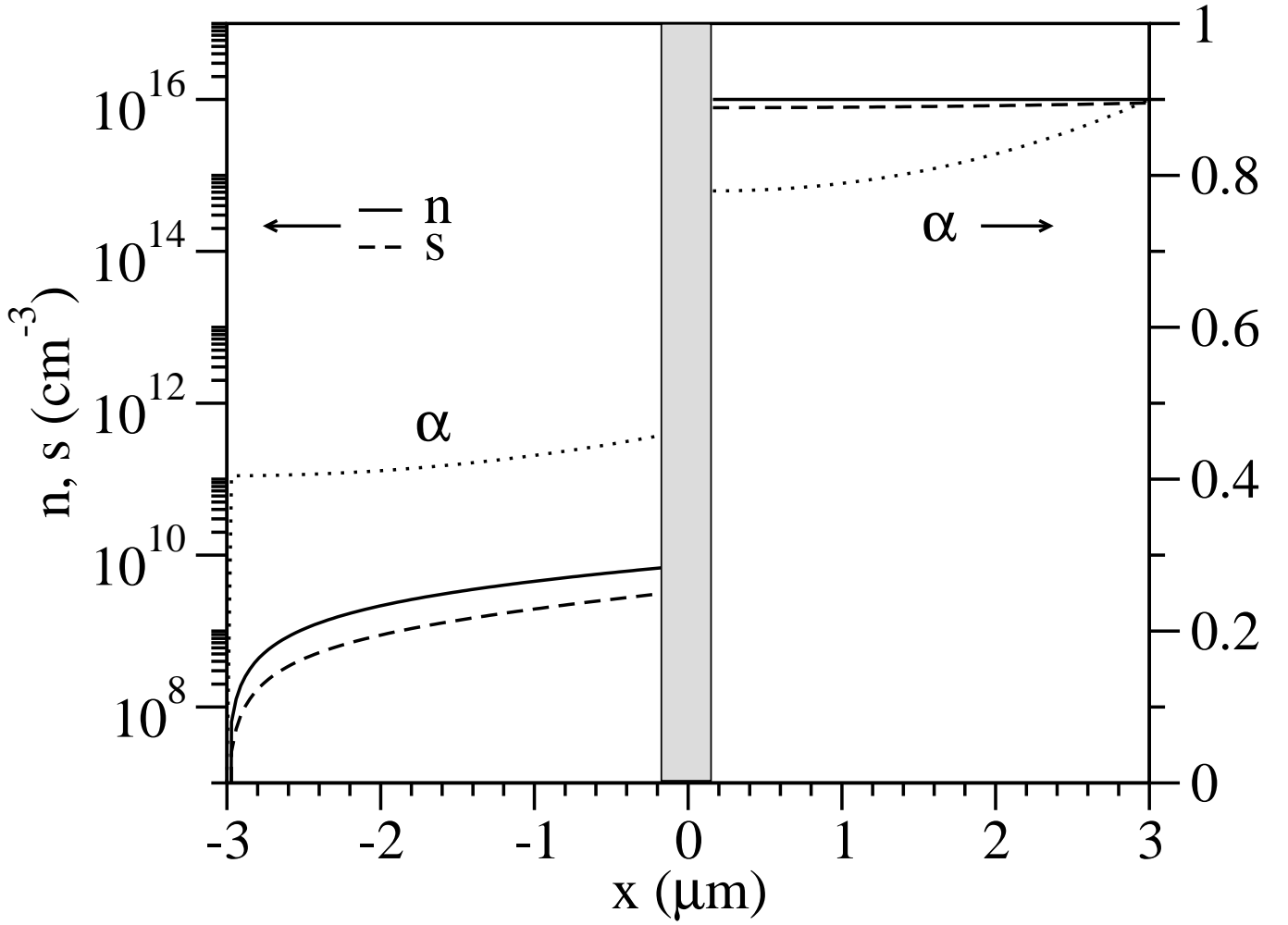


FIG. 2: An example of the majority carrier spin injection through the depletion layer (shaded). Shown are the spatial profiles of the electron (solid) and spin (dashed) densities in the magnetic p-n junction described in the text, with $\mu_{0R} = 0.5$, $\mu_{0n} = 0.4$ (the p region is nonmagnetic and the left electrode remains Ohmic), and forward bias $V = +0.8$ volt ($\approx 32 k_B T$). The left vertical axis is for the densities, while the right axis is for the spin polarization, which is represented by the dotted lines labeled with α .

$$s_L = n_{0L} e^V \frac{\mu_{0R}}{1 + \frac{\mu_{0R}^2}{2}}; \quad (57)$$

and for the spin polarization

$$\alpha_L = \frac{\mu_{0R}}{1 + \frac{\mu_{0R}^2}{2} + \frac{\mu_{0R}}{\mu_{0n}}}: \quad (58)$$

If the source spin has the same direction of polarization as the equilibrium spin in the n region, the electron density n_L , and thus the current through the junction, is reduced. If they are antiparallel, n_L and the current are enhanced. Neither spin polarization, μ_{0R} nor μ_{0L} , depends on V (except for a small dependence through w_n), being the same for forward and reverse biases. In nonmagnetic junctions ($\mu_{0R} = 0$), all the nonequilibrium spin polarization is transferred to the minority region, $\alpha_L = \mu_{0R}$, where the nonequilibrium spin has no effect on charge and current, since $n_L = n_{0L} \exp(V)$. This case has been studied numerically for a realistic model of a spin-polarized nonmagnetic p-n junction.⁵²

The reason for the absence of spin injection through the depletion layer from a magnetic n region to the nonmagnetic p region, without a source spin, is the balance between the carrier densities and thermally activated processes of forward conduction. Let the n region be positively magnetized, so that there are more spin up than spin down electrons. For a nondegenerate statistics, the number of spin up (down) electrons depends on the spin splitting ($2\mu_{nn}$) of the band as $\exp(\mu_{nn})$ [$\exp(-\mu_{nn})$]. In the forward transport, electrons need to be thermally activated to cross the barrier of the

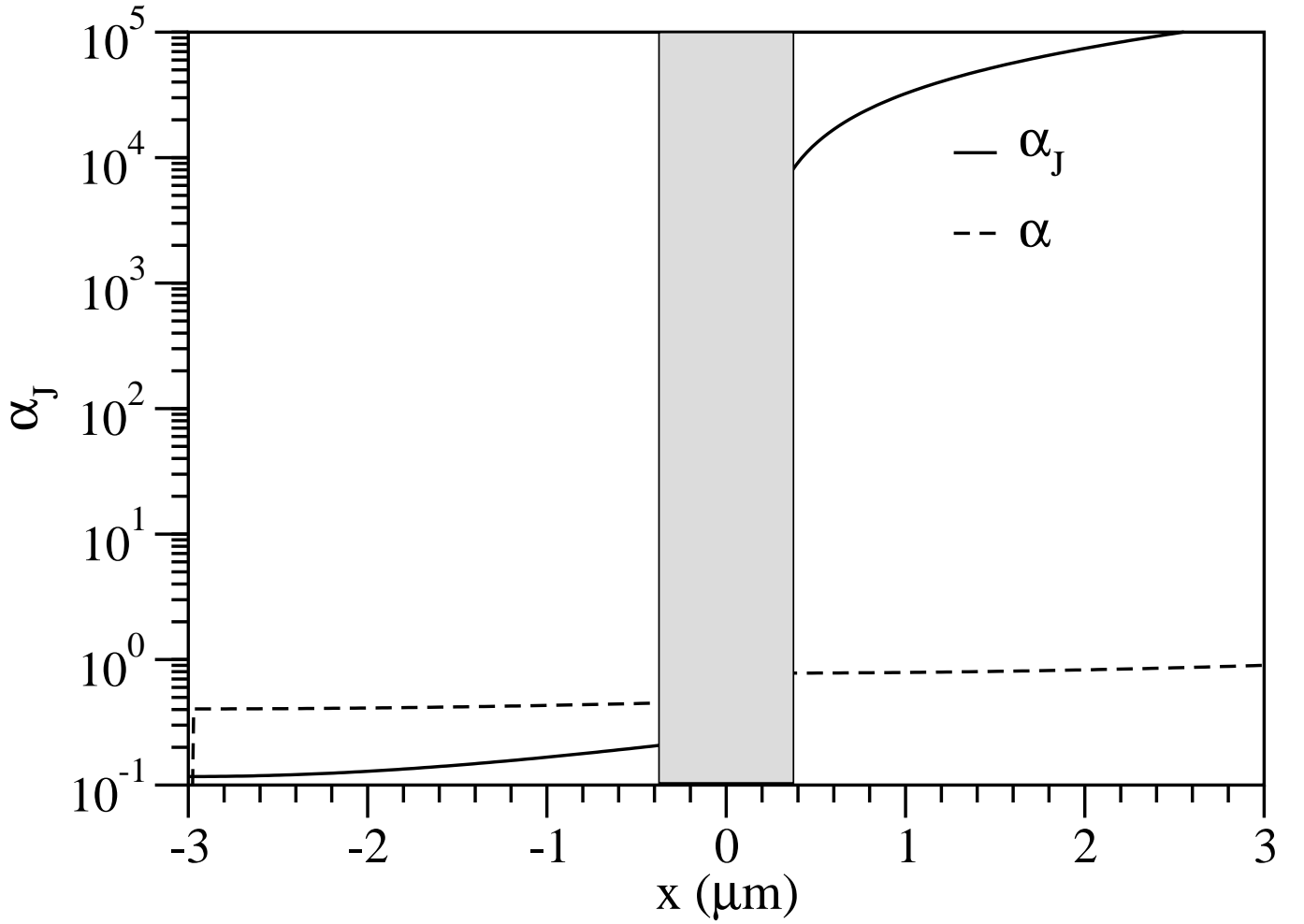


FIG. 3: Calculated current spin polarization for the majority carriers spin injection. The same parameters as in Fig. 2 apply. Both the current spin polarization α_J and the density spin polarization α are shown for comparison. The current spin polarization is enormous in the n region, decreasing upon reaching the depletion layer, and staying smaller than α in the p region.

built-in voltage lowered by the external bias. The barrier height is, however, different for spin up and down electrons. Indeed, spin up (down) electrons have the barrier higher (lower) by μ_{nn} , leading to the modulation of the transport rate by $\exp(-\mu_{nn})$ [$\exp(\mu_{nn})$]. These exponential factors exactly balance the modulation of the carrier densities. As a result, there is no difference between the transfer rates (density times the thermal activation probability) for the spin up and spin down carriers, the spin up and spin down currents are equal, and there is no spin current at R (and, by the continuity of the spin current also at L) and thus no spin injection into the minority region.

Figure 2 shows the electron and spin densities, using our model equations (Table II), for the GaAs magnetic junction example, with $\phi_R = 0.5$ and $\phi_n = 0.4$, and a forward bias of $+0.8$ volts. Spin injection into the minority region is very effective; ϕ_L is slightly greater than ϕ_R [due to the denominator in Eq. (31)]. A comparison between the current spin polarization (the profile is the same as for the spin current J_s) and the density spin polarization is in Fig. 3. The current polarization is huge at the point of spin injection, since in order to reproduce the spin polarization ϕ_n by electrical spin injection (which would depend essentially on α_J , see Sec. IV D), α_J would need to be that large. This is of course not possible, since electrical spin injection from a ferromagnetic electrode provides $\alpha_J < 1$, since α_J in ferromagnets is close to the density polarization there. The current polarization decreases upon approaching the depletion layer, since there the spin current decreases in order to be equal to the spin current at L, which is driven by the much smaller density of the minority electrons. Figure 4 shows the chemical potential profiles for the case. The chemical potentials are chosen to be zero (similarly to ϕ) at $x = w_n$ in the spin unpolarized (but biased) junction, so that at $x = w_p$ they are ϕ if the contact is Ohmic, as is the present case. This is the cause of the rapid decrease of the ϕ 's to $\phi = \phi$ at $x = w_p$. Spin injection in this graph is visible from the finite value of ϕ (which becomes

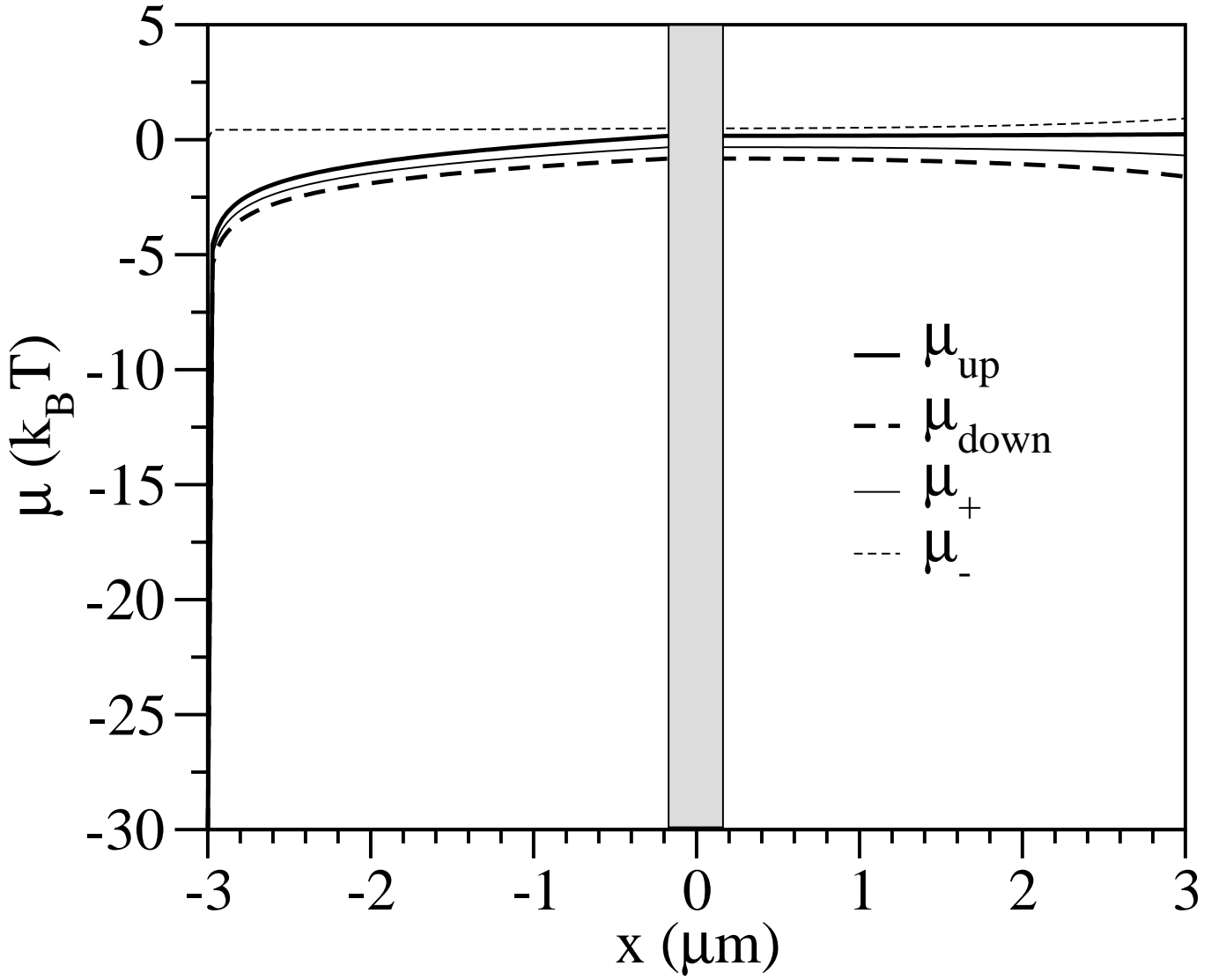


FIG. 4: Calculated chemical potential profiles in a magnetic p-n junction under the majority carrier spin injection regime. The same parameters as in Fig. 2 apply. The chemical potentials are expressed in the units of $k_B T$.

zero only in the very proximity of the left contact) in the p region.

B. Spin pumping by the minority carriers

If large (source) spin density is externally injected along with the carrier density into the minority region, the nonequilibrium spin can reach the depletion layer and be swept by the built-in electric field to the majority side, where it accumulates. We have named this effect minority electron spin pumping,^{52,53} since the spin accumulation (which is also a spin amplification, considering that the resulting spin in the majority region is much larger than that in the minority region) depends on the intensity of the spin current of the minority carriers. The faster the carriers arrive at the depletion layer, the more spin accumulates in the n side. In effect, this is an analogue of the optical spin pumping in the majority region,⁴ except that the role of circularly polarized light is played by the spin polarized minority carriers.

As an illustration consider a nonmagnetic spin-polarized p-n junction ($\phi_L = \phi_R = 0$). Let the carrier and spin densities at the left electrode only be out of equilibrium: $n_p, s_p \neq 0$. This happens, for example, when a junction is illuminated by circularly-polarized light (like in a spin-polarized solar cell⁵³) or if the junction is part of a spin-polarized junction transistor, in which case the left electrode simulates the action of the emitter. Equation (36) gives

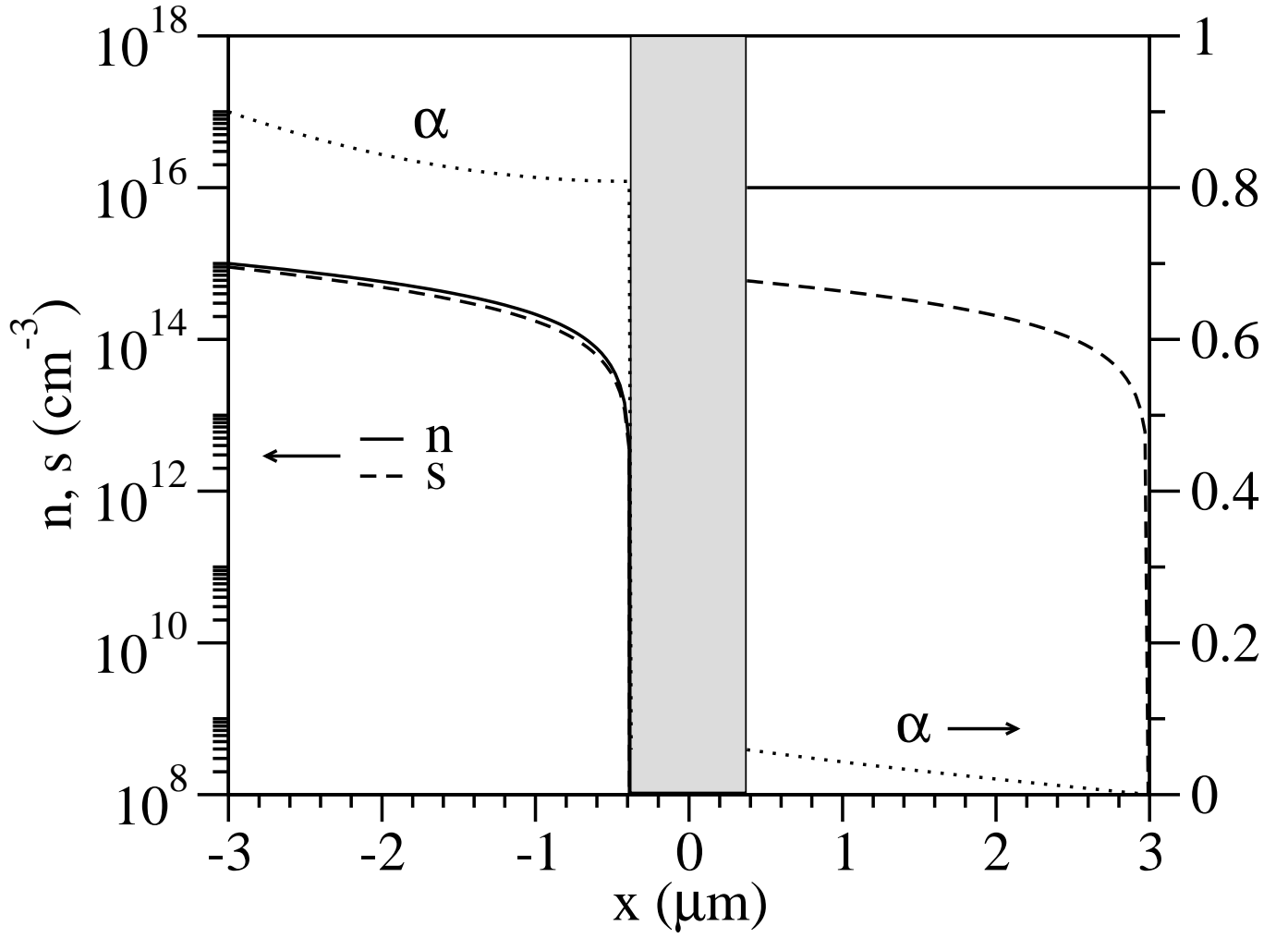


FIG. 5: An example of a minority carrier spin pumping through the depletion layer. The junction is nonmagnetic, but spin-polarized, and the carrier and spin source is placed at the left electrode, giving $n_p = 1 \cdot 10^{15} \text{ cm}^{-3}$ and $s_p = 1 \cdot 0.9 \cdot 10^{15} \text{ cm}^{-3}$ ($p_p = 0.9$). A reverse bias of 0.8 volts is applied (increasing the width of the depletion layer compared to Fig. 2).

the "pumped" spin polarization in the majority side as

$$s_R = \frac{D_{np}}{D_{nn}} \frac{L_{sn}}{L_{sp}} \frac{\tanh(w_n = L_{sn})}{\sinh(w_p = L_{sp})} s_p : \quad (59)$$

For a large majority region, $w_n \gg L_{sn}$, the injected spin is (below only holds if $w_p \ll L_{sp}$) $s_R = (D_{np}/D_{nn})(L_{sn}/w_p) s_p$, while for a short majority region, $w_n \ll L_{sn}$, the injected spin is $s_R = (D_{np}/D_{nn})(w_n/w_p) s_p$. The amount of the pumped spin polarization, relative to the amount of the source polarization is

$$\frac{s_R}{s_p} = \frac{D_{np}}{D_{nn}} \frac{L_{sn}}{L_{sp}} \frac{\tanh(w_n = L_{sn})}{\sinh(w_p = L_{sp})} \frac{n_p}{N_d} : \quad (60)$$

Spin pumping is most effective when the p region is short, $w_p \ll L_{sp}$, when

$$\frac{s_R}{s_p} = \frac{D_{np}}{D_{nn}} \frac{\min(L_{sn}, w_n)}{w_p} \frac{n_p}{N_d} : \quad (61)$$

If both L_{sn} and w_n are significantly greater than w_p , the pumped spin (and even the spin polarization) can be comparable to the source spin (source spin polarization).

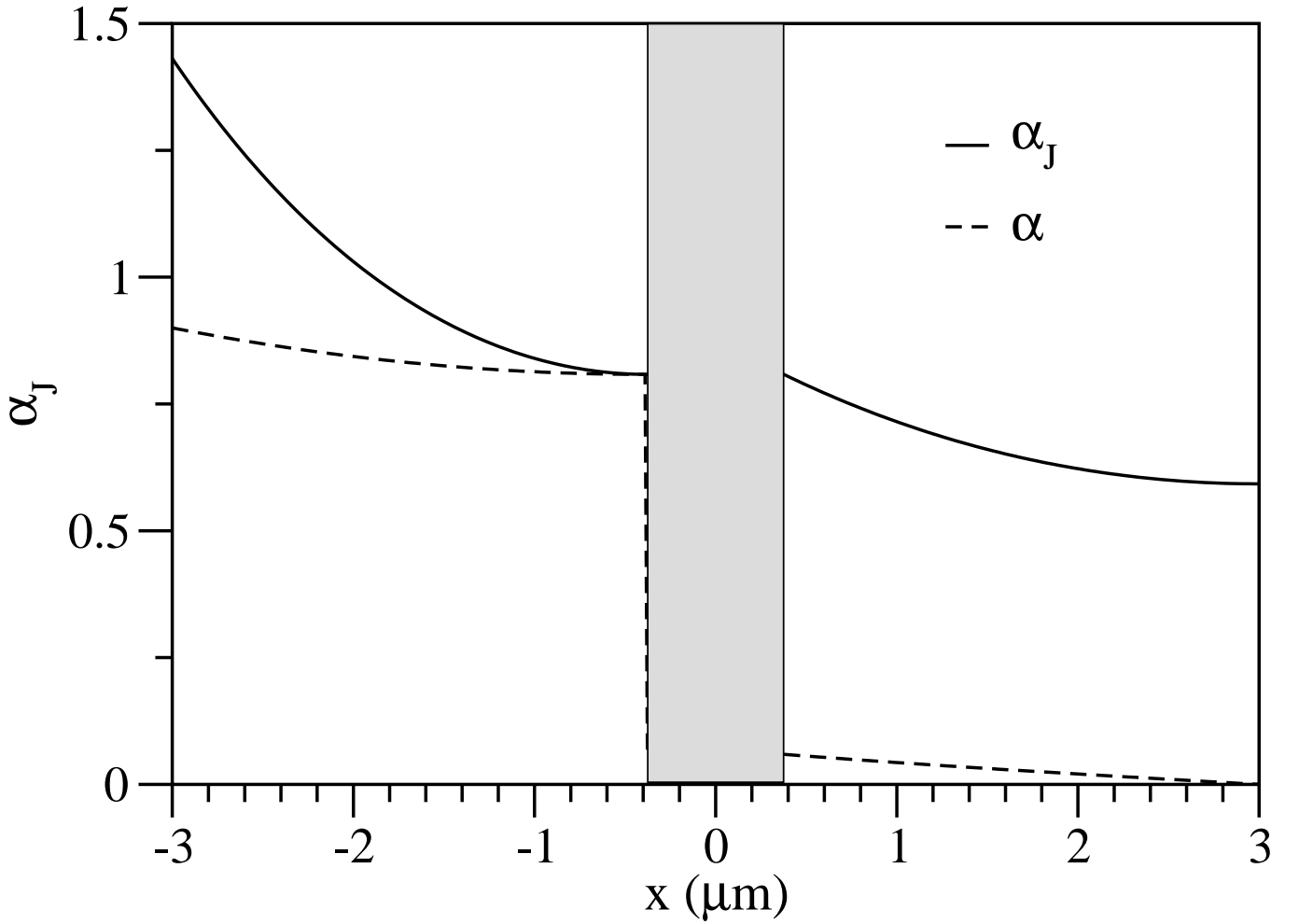


FIG. 6: Calculated current spin polarization in the minority spin pumping regime. Both current, α_J , and density, α , spin polarization profiles are shown. The current spin polarization starts at a value larger than 1 at $x = -w_p$, remains constant across the depletion layer where the spin current continuity is assumed, and decays somewhat in the n region, where its magnitude is much larger than that of density spin polarization.

A qualitative argument for the spin pumping is as follows. In the minority (p) side, the spin current goes roughly as $D_{np} \nabla_x s_p = w_p$, where we chose the largest spin in the region (being the source spin s_p) and the smallest length scale for the spin decay (here w_p). On the n side the spin current, along similar reasoning, would be $D_{nn} \nabla_x s_R = L_{sn}$, where s_R is the largest spin in the region and we chose L_{sn} to be the smallest length scale. Equating the two currents gives Eq. (61). Put in words, spin carried by the minority carriers arriving at the depletion layer is swept into the majority region by the large built-in field. In the majority region the spin both diffuses away and relaxes. In a steady state, the incoming spin flux must equal the outgoing diffusion and relaxation, which are proportional to the spin density, so that the greater is the spin influx, the greater the spin density.

A numerical example is shown in Fig. 5. The source carrier and spin densities are $n_p = 10^{15} \text{ cm}^{-3}$ and $s_p = 0.9 \cdot 10^{15} \text{ cm}^{-3}$ (the spin polarization $p = 0.9$). The junction is under reverse bias of 0.8 volts (note the increase width of the depletion layer compared to Fig. 2). The pumped spin polarization s_R is about 5%. In our numerical example all the length scales involved are comparable (roughly 3 μm), diffusivities uniform ($D_{np} = D_{nn}$) so $s_R \approx s_p$. In Fig. 6 we plot the current spin polarization α_J to demonstrate that it significantly differs from the density spin polarization α . In this example α_J is larger than 1 at the left electrode due to the chosen boundary conditions, and in the n region it is much greater than the density spin polarization. The chemical potential profiles for the case are shown in Fig. 7. In the majority region ϕ_+ nearly vanishes, while $\phi_- \approx \phi_{\#}$, demonstrating a positive net nonequilibrium spin polarization in the n region. The small magnitudes of the nonequilibrium chemical potentials in the majority region still yield large spin density, since they appear in the exponent which multiplies the equilibrium carrier density, which is large in the majority region (and small in the minority, where the chemical potentials have

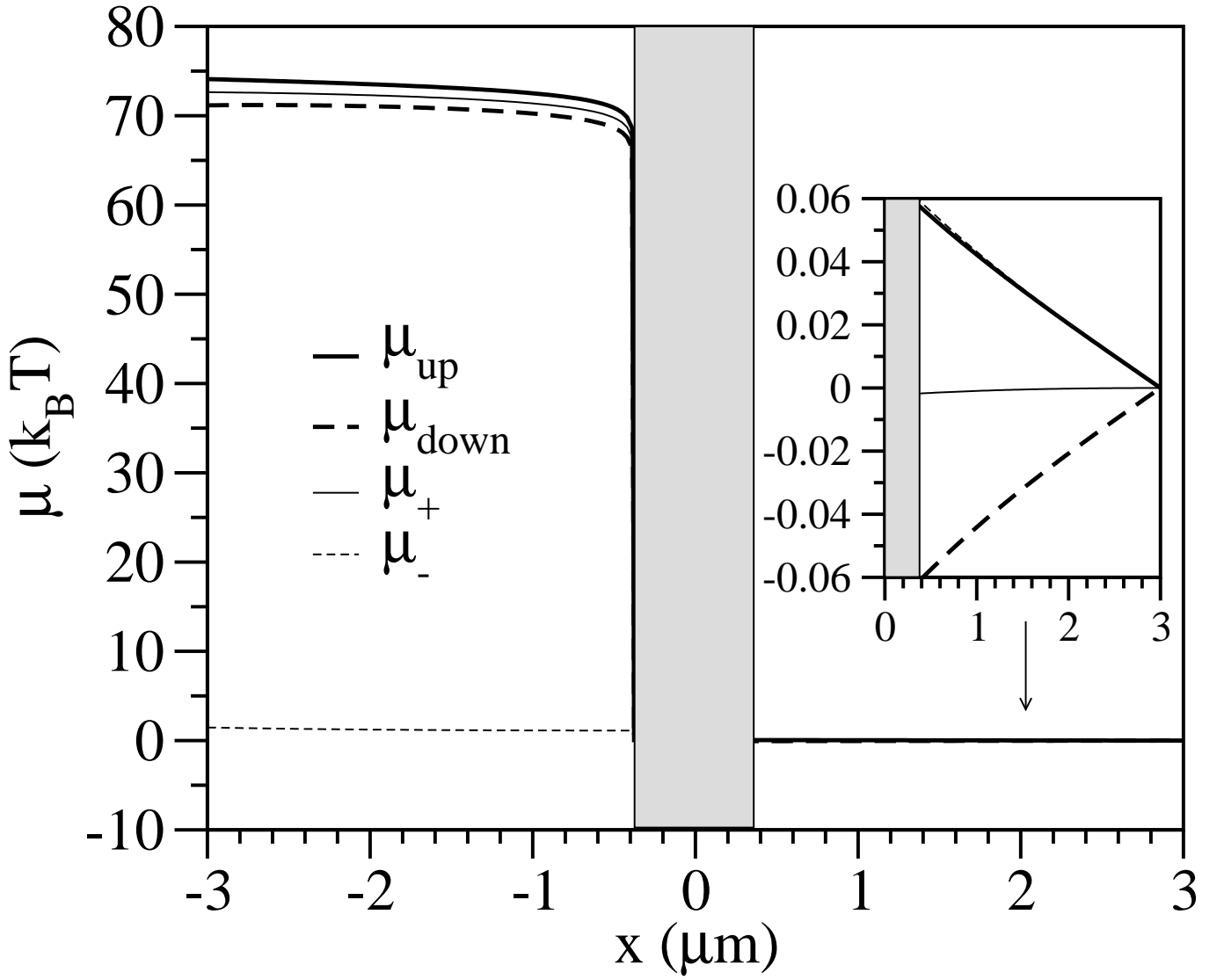


FIG. 7: Calculated chemical potential profiles in a nonmagnetic spin-polarized p-n junction under the minority carrier spin pumping regime. The parameters as in Fig. 5 apply. The input shows the majority region values on a scale where different μ 's are visible.

accordingly large magnitudes).

C. The spin-voltaic effect

A spin-voltaic effect is a generation of charge emf for current by nonequilibrium spin. A first realization of the spin-voltaic effect was the Silsbee-Johnson spin-charge coupling^{85,86} in a ferromagnetic/nonmagnetic metal interface with nonequilibrium spin injected into the nonmagnetic metal. The emf across the interface arises due to the difference in the chemical potentials in the two metals, with different effects on the different spin states. Analogous phenomena can occur in many other hybrid systems (semiconductor/metal or semiconductor/semiconductor). Here we describe a specific realization of the spin-voltaic effect in magnetic p-n junctions, where the role of the interface is played by the depletion layer.

Consider a magnetic/nonmagnetic p-n junction, with the p region magnetic ($n_p = 0$) and the n region nonmagnetic but spin polarized ($n_n \neq 0$). No external bias is applied ($V = 0$). It follows from Eq. (36) that

$$R = \frac{n}{\cosh(w_n = L_{sn})}; \quad (62)$$

which is the same as Eq. (55) (simply expressing the fact that the polarization is bias independent). As a result, there will be nonequilibrium carrier and spin densities in the minority region [see Eq. (32) and (33)]:

$$n_L = n_{0L} \frac{\phi_L}{\phi_R}; \quad (63)$$

$$s_L = n_{0L} \frac{\phi_L}{\phi_R}; \quad (64)$$

The nonequilibrium minority carrier density n_L leads to the minority diffusion and relaxation, and thus to the charge current (or voltage in an open circuit). The spin-voltaic current is [see Eq. (43)]

$$j_h = j_{gn} \frac{\phi_L}{\phi_R}; \quad (65)$$

The current is of the order of the generation current, and changes sign with reversing either the magnetic field (which reverses ϕ_L) or the orientation of the source spin s_n . Neglecting the variation of ϕ_R with bias (through w_n), the open circuit voltage for the spin-voltaic effect is obtained by requiring that j vanishes:

$$V_{oc} = \frac{k_B T}{e} \ln \left(1 + \frac{j_{gn}}{j_{gp}} \frac{\phi_L}{\phi_R} \right); \quad (66)$$

The voltage, which is typically of the order of $k_B T$, is negative (reverse biasing) if the polarizations are parallel, and positive (forward biasing) if they are antiparallel. The spin-voltaic effect here is similar to the photovoltaic effect, where the photocarriers generated within the carrier diffusion length L_{np} of the depletion layer are swept by the built-in field to the majority side, generating photocurrent. A spin-voltaic effect arises if nonequilibrium spin is generated within the spin diffusion length L_{sn} of the depletion layer, disturbing the balance between the generation and recombination currents.

Indeed, in equilibrium both the generation and the recombination currents in a magnetic p-n junction are equal and there is no net charge flow. Let ϕ_L be positive. Then the barrier for the majority electrons to cross the depletion layer (see Fig. 1) is smaller for spin up than for spin down electrons. If the spin in the majority region is driven out of balance (without applying an external bias), then the delicate balance of the generation and recombination currents is disturbed, resulting in a net charge current. Increasing the number of spin up majority electrons, for example, increases the recombination current, since more electrons have now a smaller barrier to cross (the generation current does not depend on ϕ_R or bias). In our geometry, the net electron flow is forward (from the right to the left, $j_h > 0$). If, on the other hand, we increase the number of spin down electrons, more electrons have now a higher barrier to cross, reducing the recombination current, resulting in a net reverse flow (from the left to the right, $j_h < 0$). The spin-voltaic effect is the reason for the giant magnetoresistance of magnetic p-n junctions,⁵⁴ since when a bias V is applied, the spin-voltaic current grows as $\exp(V)$, similarly to the normal rectification current.

The spin-voltaic effect is illustrated in Figs. 8-11. First consider parallel spin polarizations, $\phi_L = \phi_n = +0.9$. There is no bias, $V = 0$. The carrier and spin densities and the spin polarization are plotted in Fig. 8. The induced nonequilibrium spin and charge in the p region are greater than the equilibrium values, leading to a forward current of electrons. The spin polarization is also higher than in equilibrium. The chemical potential profiles are shown in Fig. 9. If the spin polarization of the source spin is reversed, $\phi_L = \phi_n = -0.9$, the carrier and spin densities and the spin polarization decrease in the minority region, leading to a reverse electron current. The density profiles for this case are in Fig. 10, and the chemical potentials are plotted in Fig. 11.

Let the magnetic field B controls the conduction band spin splitting. Then $\phi_0(B) = \phi_0(-B)$. Keeping ϕ_R as an independent (of B) parameter, the direction reversal of the magnetic field results in a change in charge current:

$$j_h(B) - j_h(-B) = j_{gn} \frac{n_L(B) - n_L(-B)}{n_{0L}}; \quad (67)$$

This is a realization of giant magnetoresistance (GMR) in magnetic diodes. The relative change of the charge current upon reversing the direction of magnetic field (while keeping ϕ_R unchanged) can be measured by the giant magnetoresistance parameter, here denoted as β :

$$\beta = \frac{n_L(B) - n_L(-B)}{n_L(B)}; \quad (68)$$

which at forward bias and $\exp(V) \gg 1$, in terms of the known parameters, can be expressed as

$$\beta = 2 \phi_R \frac{\phi_L}{1 + \frac{\phi_L}{\phi_R} + \frac{\phi_R}{\phi_L}}; \quad (69)$$

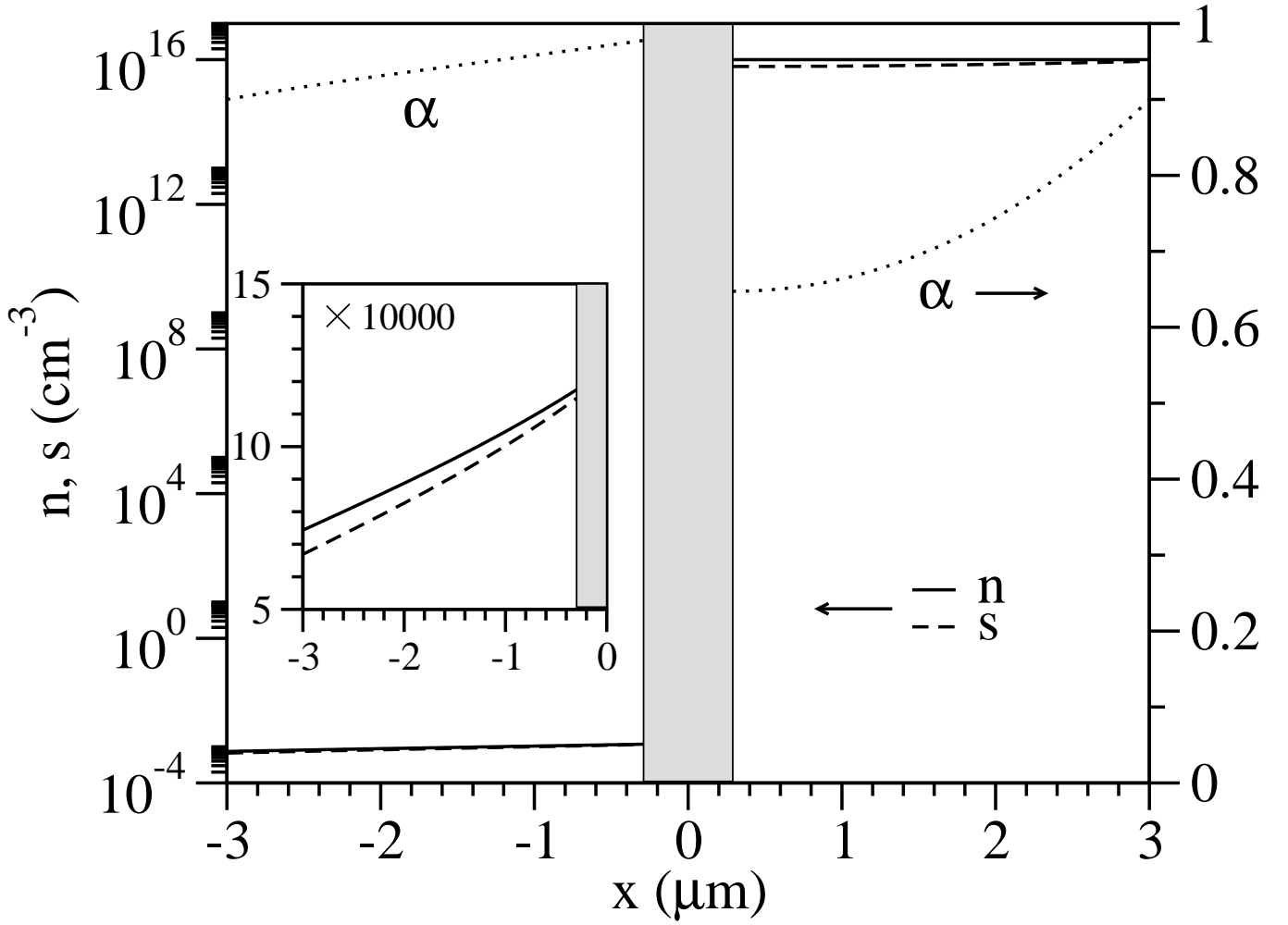


FIG. 8: The spin-voltaic effect in a spin-polarized magnetic p-n junction. Shown is a junction with a magnetic p region ($\phi_L \neq 0$) and a nonmagnetic n region ($\phi_R = 0$). No bias is applied. Both electrodes are Ohmic, except that there is a spin source at $x = w_n$. In the example $\phi_L = +0.9$ and $\phi_n = +0.9$. The carrier and spin densities in the p region are very close to the equilibrium values, with a small variation due to the nonequilibrium spin. The inset shows this variation on a 10000 times increased scale. Both densities are higher than in equilibrium, leading to a forward charge current.

The GMR effect is possible only in magnetically inhomogeneous p-n junctions with nonequilibrium spin. As a special case consider the p region magnetic ($\phi_R = 0$). Then

$$\beta = \frac{2 \phi_R \phi_L}{1 + \phi_R \phi_L} : \quad (70)$$

This case is a semiconductor analogue of the Silsbee-Johnson spin-charge coupling,⁸⁵ where a spin emf arises from the proximity of a nonequilibrium spin in a metal and a ferromagnetic electrode. A detailed numerical study of the GMR effect in magnetic diodes can be found in Ref. 54. Putting reasonable parameters $\phi_L = 0.5 = \phi_R$, Eq. (70) gives $\beta = 2/3$, which is a 66 % GMR. A more optimistic set, $\phi_L = 0.9 = \phi_R$, leads to $\beta = 8/5$, or a 850 % GMR, demonstrating a great technological potential of magnetic p-n diodes.

D. Spin injection by the biasing electrode

Thus far s_n was a free input parameter of the model. If, however, the biasing electrodes themselves can inject spin (for example if they are magnetic), then the source spin density will not be a good starting boundary condition. We consider an example of the source spin injection by the right electrode into the nonmagnetic majority, n, region, keeping only the p region magnetic. We assume the model in which the spin current across the electrode/n-region

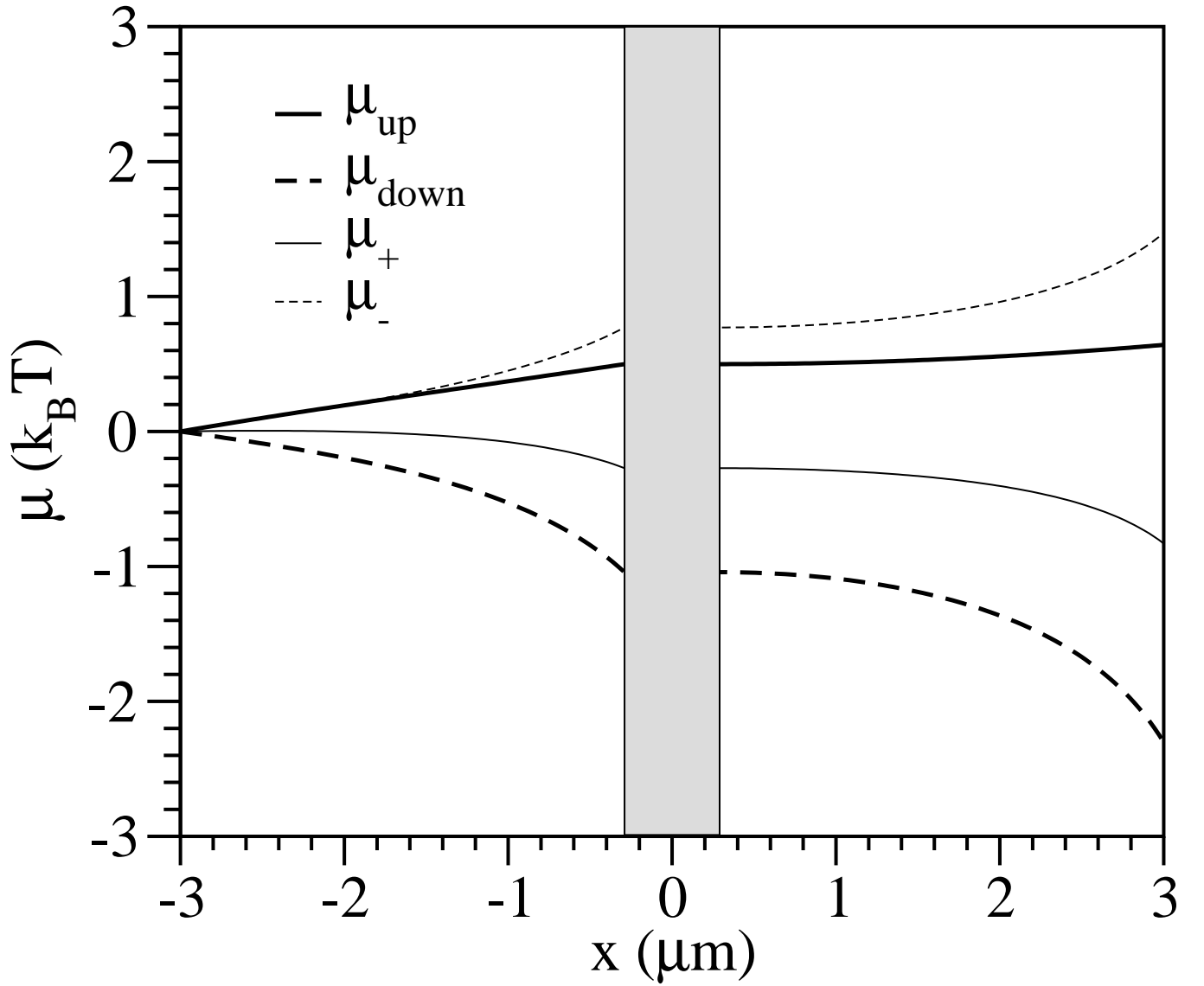


FIG. 9: Calculated chemical potential profiles in a spin-polarized magnetic p-n junction under the conditions specified in Fig. 8.

interface is preserved. In this scenario the boundary condition at $x = w_n$ reads (all the current at the contact is carried by electrons, since the hole density is in equilibrium there)

$$j_{sn} = j_n j; \quad (71)$$

where $j_{sn} = qD_{nn}(w_n)$ and $j_n = j(w_n)$ is the spin injection efficiency (here the current spin polarization at the contact) equal, in an ideal case, to the spin polarization in the electrode material reduced by interface spin relaxation. Our strategy is to convert this boundary condition to the condition on the spin density: We calculate s_n as a function of $j_n j$ and then use the formulas derived earlier to obtain the charge current in a self-consistent manner (this is needed because the boundary spin depends on the current which, in turn, is calculated using the boundary spin). Equation (20) gives

$$j_{sn} = \frac{qD_{nn}}{L_{sn}} \frac{s_n \cosh(w_n/L_{sn})}{\sinh(w_n/L_{sn})} s; \quad (72)$$

If we further assume that the left contact is ohmic, by substituting Eq. (55) for s , the above equation can be solved for the source spin density with the result

$$s_n = \frac{j_n j L_{sn}}{qD_{nn}} \coth \frac{w_n}{L_{sn}} \frac{2s_0 L e^V}{\tanh^2(w_n/L_{sn})} \frac{1}{1}; \quad (73)$$

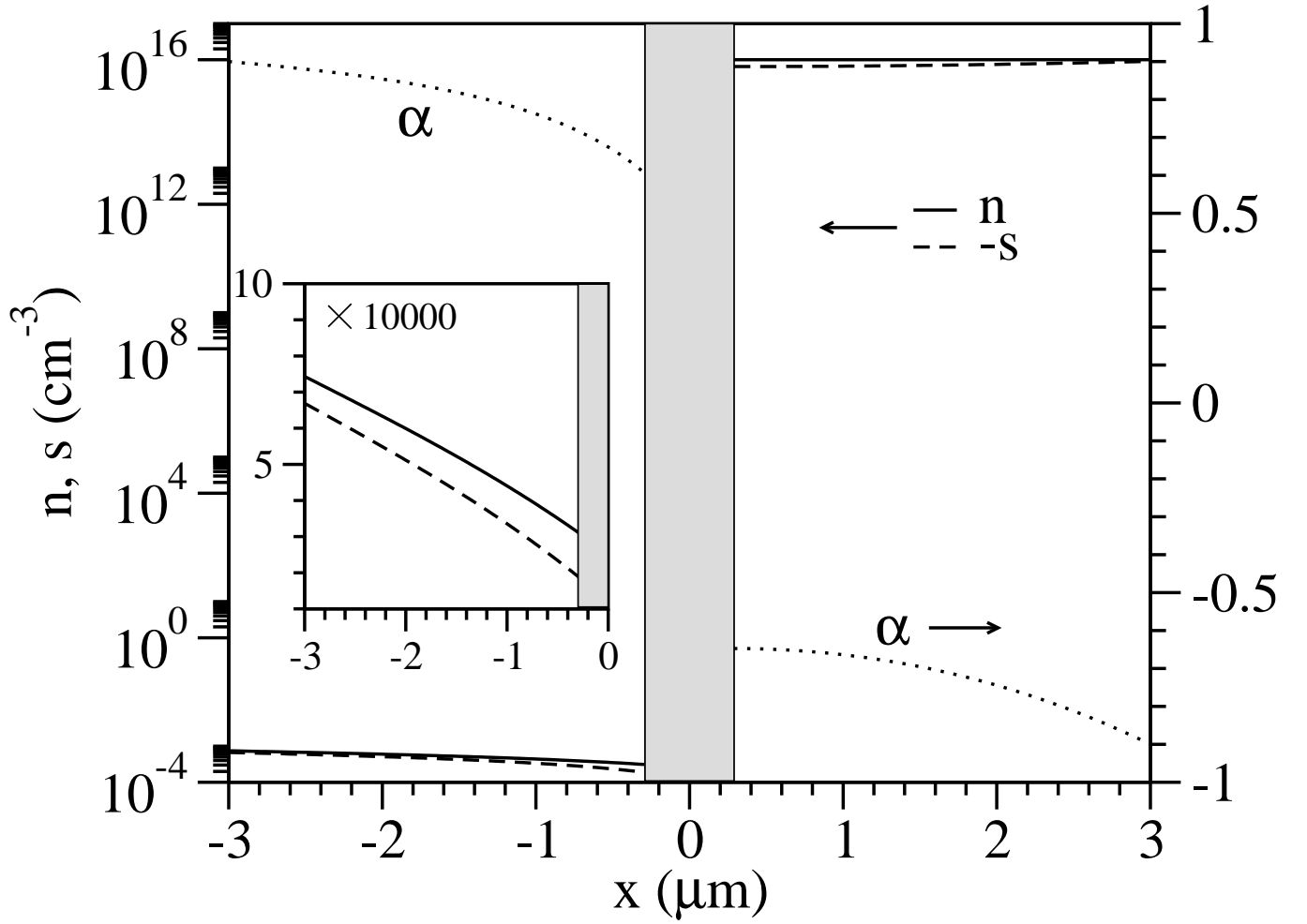


FIG. 10: The spin-voltaic effect in a spin-polarized magnetic p-n junction. The same conditions as in Fig. 8 apply, but the direction of the source spin is reversed, $s_n = -0.9$. The figure shows the negative spin density (s) in the n region (and normal in the p side). The carrier and spin densities have values close to the equilibrium ones, but are now somewhat smaller, due to the presence of the antiparallel nonequilibrium spin. This density variation, which is seen in the inset on a 10000 times greater scale, leads to a reverse charge flow.

The nonequilibrium spin polarization at the depletion layer then is

$$s_R = j_n j_p \frac{L_{sn}}{qD_{nn}} \frac{1}{\sinh(w_n = L_{sn})} \frac{1}{4s_{0L}} e^V - 1; \quad (74)$$

where another geometric/transport parameter is introduced:

$$\alpha = \frac{3}{\tanh^2(w_n = L_{sn})}; \quad (75)$$

In a first approximation one can put $j = j_n + j_p$ for the current in Eq. 74. The injected spin s_R is then of the order of the minority electron density times $L_{sn} = L_{np}$. This is generally larger than the spin extraction factor coming from the term with α , but still small to lead to a significant modulation of nonequilibrium spin. The charge current is obtained by solving Eq. (47) for j , with s_R from Eq. 74. The result is

$$j = (j_p + j_{0n}) (1 + j_n \alpha_{0L}) - \alpha_{0L} j_{gn} e^V - 1 \frac{s_{0L} e^V}{N_d}; \quad (76)$$

where

$$\alpha_{0L} = \alpha_{0L} \frac{j_{gn} e^V}{N_d} \frac{L_{sn}}{qD_{nn}} \frac{1}{\sinh(w_n = L_{sn})}; \quad (77)$$

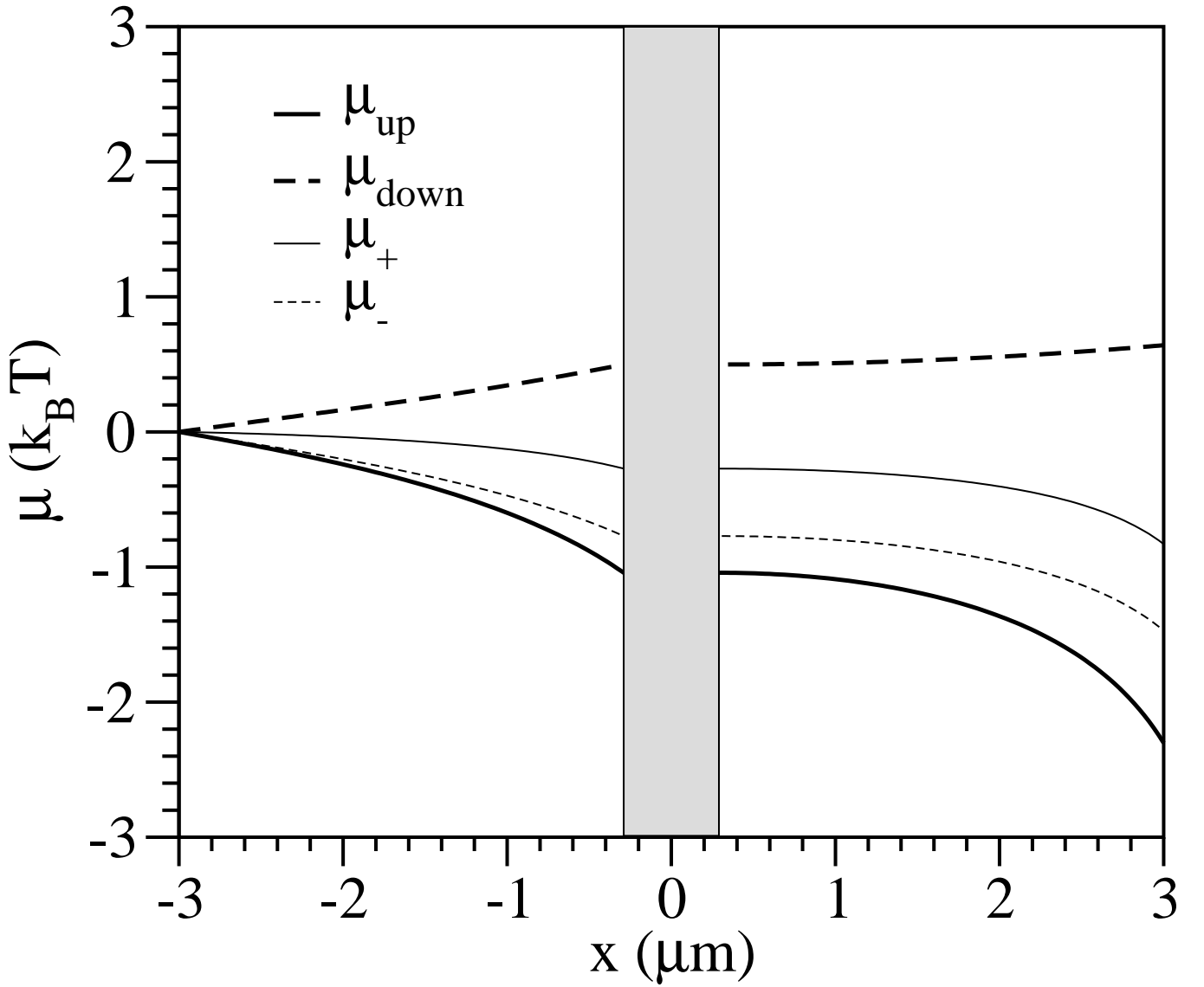


FIG. 11: Calculated chemical potential profiles in a spin-polarized magnetic p-n junction. The same parameters as in Fig. 10 apply.

Unlike in the case of independent external spin source, the spin injected by the biasing electrode is very small, because of the small current flowing in the junction (the current is carried by the minority carriers), so that only a small spin current can build up the source spin. As a result, the spin injected from the contact has a very small effect on the charge properties of the junction. Charge current, in particular, is only slightly modified from the spin-equilibrium value of $j = j_p + j_n$. The spin-voltaic effect is absent (except for the small effect caused by spin extraction), since at zero bias no nonequilibrium spin is injected. Nevertheless, even if small, the I-V characteristics modification should be observable at reasonably large biases, and could be used to characterize spin properties of the junction. Furthermore, the above model of spin injection, based on Eq. (71), is rather simple and we cannot exclude the possibility of a different behavior (especially more pronounced spin dependent effects) with realistic interfaces. In fact, our method shows a way how to characterize spin properties of real (electrode) interfaces by measuring charge response of the junction.

E. Spin injection and extraction at large biases

We have shown numerically in Ref. 54 that spin can be injected and extracted through the depletion layer at large biases, even with no source spin present. Significant spin injection from the magnetic n region into the nonmagnetic p region occurs at large biases and, similarly, significant spin extraction occurs from the nonmagnetic n region into the magnetic p region. These intrinsic spin injection phenomena have their origin in the low bias physics. Indeed, there is a (normally negligible) spin injection in the absence of source spins even in our theory. We have already demonstrated spin extraction in Eq. (36). If no source spin is present, then

$$s_R = -s_{0L} \exp(V) : \quad (78)$$

The nonequilibrium spin in the n region will have the sign opposite to that of the equilibrium spin in the p region. The spin is more extracted the larger the bias is. Normally, at small biases, the injected spin polarization $s_R = -s_{0L} \exp(V) = N_d$ is small (in the postulated low injection regime), but it shows the trend of spin extraction exponentially increasing with V towards the large bias regime. The reason for Eq. (78) is the continuity of the spin current across the depletion layer. Without any spin source, the spin current J_{sL} will be given by the flow of electrons with the equilibrium spin polarization s_{0L} [see Eq. (15)]. The same spin current must appear in the n region at R . For positive s_{0L} , the spin current in p is negative. In the n region, for the spin current to be also negative there must be a positive gradient of s and, since $s_R = 0$, the spin at R must be negative: $s_R < 0$.

On the other hand, our theory thus far does not predict any spin injection from the magnetic n to the nonmagnetic p region. Indeed, in the absence of source spin, and with $s_{0L} = 0$, Eq. (36) gives $s_R = 0$. To explain the intrinsic spin injection observed at large biases (but also at small biases, although on a smaller scale⁵⁴), we have to introduce electric field E into the picture. In fact, once the nonequilibrium spin becomes small compared to the equilibrium one in the majority region, even at small biases electric field cannot be neglected. We will quantify this condition below. There are two factors which need to be considered when introducing charge effects in spin transport in the bulk regions. First, we will include the electric drift force into the spin current and, second, we will explicitly account for charge neutrality by postulating that $n = N_d + p$ (instead of what was used thus far, $n = N_d$). These two factors can be normally neglected at small biases, but here we use them to demonstrate the trends, namely the spin injection, which will become important at large V .

Including the E -field and the charge neutrality, the spin diffusion equation from Eqs. (2) and (4) becomes

$$s'' + E s' = \frac{s}{L_{sn}^2} - \frac{p}{L_{sn}^2} : \quad (79)$$

We have neglected the nonlinear term $s \cdot \nabla p$, justifiably if $(T_1 = p_n) / (p = N_d) \ll 1$, which is quite generally the case at low injection. The above equation needs to be supplemented with the diffusion equation for holes,

$$p'' = \frac{p}{L_{pn}^2} : \quad (80)$$

In Eq. (79) the term with the first derivative comes from the electric drift, while the term proportional to p appears because of the neutrality condition $n = N_d + p$. The latter term acts as an intrinsic spin source, similarly to the term of n in the spin diffusion equation (11) for the minority electrons. The neutrality condition also guarantees that the electric field is uniform ($E' = 0$). Equation (79) has already been considered and solved^{55,56,94} without the intrinsic source term, which becomes important in bipolar transport at large biases. For completeness, we present the full solution to Eq. (79), as well as the spin current profile, in Appendix C.

The full analysis in Appendix C shows that at least for $L_{pn} \ll L_{sn}$, the contribution from the charge neutrality ($n = p$), that is, from the hole density effects in spin transport, can be neglected. In the opposite case, the contribution would lower s_R , as can be seen easily by equating J_{sR} in Eq. (C8) to zero. The electric field, on the other hand, increases s_R , ultimately leading to spin injection at large biases. Indeed, from Eq. (C8) one obtains for spin injection from the majority magnetic region to the minority nonmagnetic region in the absence of source spin, but at a finite bias,

$$s_R = s_R(L_{se} E) \tanh \frac{w_n}{L_{se}} : \quad (81)$$

To obtain E we can use the carrier current continuity across the depletion layer: $J_{nL} = J_{nR}$, where J_{nL} is given by Eq. (10) and $J_{nR} = D_{nn} (N_d E - \frac{p}{R})$, with p calculated in Appendix C. We get

$$E = \frac{R}{N_d L_{pn}} \coth(w_n = L_{pn}) + \frac{D_{np}}{D_{nn}} \frac{n_L}{N_d L_{np}} \coth(w_p = L_{np}) : \quad (82)$$

The electric field is positive at forward biases, making s_R and thus s_L is of the same polarity as s_{0R} . This explains the large bias spin injection (and the increase of spin polarization in the magnetic n region) observed in Ref. 54. The electric field spin injection will also happen at small biases, but, because the field is very small ($n_L \approx N_d$; $p_R \approx N_d - 1$), the spin injection is negligible. However, the $E - s_L$ must be considered in cases where spin injection due to source spin leads to s_R as small as n_L .

Equation (82) yields the criterion for neglecting electric drift in spin transport in the n region (which is in contrast to the majority carriers, for which electric drift cannot be neglected). Indeed, one needs to compare the typical magnitudes of the spin drift ($s_R E$) with the spin diffusion ($s = L_{sn}$), to obtain

$$E (s_{0R} + s_R) \leq s_R = L_{sn} : \quad (83)$$

For a nonmagnetic n region ($s_{0R} = 0$) this is always the case, since $E L_{sn} \ll 1$ because of low injection (and reasonably assuming that the spin diffusion length is not much greater than the carrier diffusion lengths). For the magnetic region, the above condition is satisfied if $s_R \leq (E L_{sn}) s_{0R}$, which roughly means that the nonequilibrium spin in the n region (appearing through the spin source, for example) should be greater than the nonequilibrium carrier density times the ratio of the spin diffusion length to the carrier diffusion length. This is well satisfied in the low injection regime, where the nonequilibrium carrier densities are small enough (even if L_{sn} would be one to three orders of magnitude greater than the carrier diffusion lengths). However, the condition (83) places the lower limit on the source spin to lead to pure spin diffusion in the n region.

Finally, the neglected spin relaxation current $J_{s,relax}$ also contributes to spin injection, more with increasing bias, since then the spin density in the depletion layer increases and with it spin relaxation. The difficulty in introducing $J_{s,relax}$ is that it depends on both bias and s_R complicating the self-consistent process of obtaining s_R in terms of the input parameters and bias. One may expect, though, that spin relaxation processes in the depletion layer will decrease the spin injection efficiency (that is, reduce s_L) while allowing for larger s_R to balance the spin current in the minority region. Our numerical calculations, which take into account the effects of $J_{s,relax}$, find that its contribution is indeed small at low biases.⁹²

F. Magnetic drift in the neutral regions

Our model and its conclusions thus far were based on magnetic p-n junctions with homogeneous magnetic doping in the neutral regions. The doping, and thus the band spin splitting and the equilibrium spin polarization, changed spatially only in the transition region. As a result, the magnetic drift force \vec{F}^0 dropped from the calculations and the inhomogeneous magnetic doping affected the results only through the equilibrium spin densities. Here we take the next step and ask how would the physics of magnetic p-n junctions be affected if, additionally, the neutral regions were inhomogeneously doped with magnetic impurities (or, to the same effect, were homogeneously doped but placed in an inhomogeneous magnetic field). We will show that magnetic drift modifies both the spin injection through the depletion layer, and the I-V characteristics of magnetic p-n junctions. The effects of \vec{F}^0 are qualitatively different in the majority and the minority regions, so we will discuss the two regions separately. Most of our discussion below applies equally to homogeneous (in relation to nonmagnetic doping) semiconductors with spin split majority and minority bands.

Consider the majority, n, region first. In the presence of an inhomogeneous spin splitting of the conduction band, the electron current in the region is

$$J_n = D_{nn} (-nE + s_{nn}^0 - n^0) : \quad (84)$$

The current must vanish in equilibrium where $n = N_d$ and $s = 0 N_d$. This is only possible if a local electric field,

$$E_0 = -\frac{1}{n} \frac{dn}{dx} ; \quad (85)$$

develops. The resulting electric drift needs to counter the magnetic drift. The existence of E_0 is also warranted by the vanishing spin (J_s) and hole (J_p) currents. In the latter the electric field needs to balance the equilibrium hole diffusion $p_0^0 [p_0$ is now spatially dependent through n_n , see Eq. (A 3)]. The field E_0 , similarly to the built-in field in the depletion layer, is an equilibrium field, not an emf, as it does not lead to a net current.

The origin of the equilibrium electric field is otherwise almost homogeneous charge situation (the majority carrier density is almost constant) can be qualitatively explained as follows. Take an n-type semiconductor doped inhomogeneously with magnetic impurities in zero magnetic field. In equilibrium the chemical potential is constant. Switch on a magnetic field. At first, the chemical potential will vary with x through n_n according to Eq. (A 7). The sample will come to equilibrium by rearranging its charge as the electrons will move in the direction of decreasing ϕ_n , resulting

in a constant chemical potential, but also in a space charge (see below) and a space electric potential opposing further electron motion. Then

$$\phi_0 = -\ln \cosh(\phi_{nn}) \quad (86)$$

The equilibrium electric field is $E_0 = -\frac{d\phi_0}{dx}$, reproducing Eq. (85) obtained from transport considerations. Electric potential ϕ_0 bends both the conduction and the valence band. As for the conduction band, ϕ_0 tends to straighten the lower spin band (say, the spin up band if ϕ_{nn} is positive) and steepen the upper spin band. At large magnetic fields the band bending of the lower spin band entirely eliminates the spatial variations of the band due to ϕ_{nn} , while these variations are doubled in the upper spin band. The valence band too is affected. Originally constant, the band acquires spatial variation ϕ_0 to balance the equilibrium hole distribution.

In turn, the inhomogeneous E_0 induces space charge ρ_0 , according to Poisson's equation: $\rho_0 = E_0' / (k_B T/q)$. In principle, both E_0 and ρ_0 need to be obtained self-consistently by solving for the equilibrium semiconductor densities taking into account Poisson's equation (this was done numerically in Ref. 54 for the transition region, where the E_0 -like field is present due to the inhomogeneous magnetic doping). However, the induced local charge density is small enough to be neglected for most practical purposes (unlike the induced charge density in the depletion region). Indeed, the induced changes in the carrier density come to $\delta n = q N_d (\phi_{nn} / D)^2 = \cosh^2(\phi_{nn})$, where $D = \sqrt{(k_B T / N_d q^2)}$ is the Debye screening length in the majority region. For GaAs with $\mu = 13D$ and at room temperature, the density is $\delta n = q \cdot 2 \cdot 10^3 (\phi_{nn} [\text{cm}^{-1}])^2 \text{ cm}^{-3}$. If the magnetic splitting changes by $k_B T$ over a micron (so that $\phi_{nn} \sim 10^4/\text{cm}$), we get $\delta n \sim 2 \cdot 10^3 \text{ cm}^{-3}$. This shows that for carrier densities greater than, say, 10^{15} cm^{-3} the induced densities in the carrier concentrations can be neglected, and Eq. (85) is a reliable estimate of E_0 . In general, the space charge can be neglected if the band splitting varies by $k_B T$ over the length scales greater than D . This is in complete analogy with space charge considerations due to the usual carrier doping.⁸⁸ Once $\phi_{nn} / D > 1$, which is normally the case when a magnetic and a nonmagnetic semiconductor form a contact for spin injection, the space charge and its distribution ($\rho_0 = q$) cannot be neglected. Indeed, for ϕ_{nn} changing over a 0.1 μm , the induced charge density is $q \cdot 10^5 \text{ cm}^{-3}$. Selective doping of semiconductors with magnetic impurities on spatial scales both smaller and larger than D can prove a useful tool for band structure and space charge engineering in designing new spintronic devices.

Expanding about the equilibrium values for the densities and the electric field, the electron and spin currents in the n region become

$$J_n = D_{nn} (N_d E - N_d \frac{d\phi_{nn}}{dx} + p_0^0); \quad (87)$$

$$J_s = D_{nn} N_d (\phi_0 E + \phi_0 \frac{d\phi_{nn}}{dx} + \phi_0^0); \quad (88)$$

where E describes only the electric field induced by the applied bias. Nonequilibrium charge neutrality, $n = p$, is assumed. In a homogeneous n-type semiconductor with finite ϕ_{nn} , maintaining a nonequilibrium spin polarization would lead to a spin emf according to Eq. (87). For a constant ϕ_{nn} , for example, the spin emf is ϕ_{nn} , where ϕ_{nn} is the drop of ϕ_{nn} across the sample. Spin injection is modified by the presence of ϕ_{nn} in Eq. (88). Considering here only a special case of a constant ϕ_{nn} and large spin polarization, $j_0 \gg 1$, the spin current at $x = 0$ is modified from Eq. (21) to

$$J_{sR} = \frac{D_{nn}}{L_{sn}} \frac{1}{2} \{ \phi_0 R + \phi_0 \frac{d\phi_{nn}}{dx} L_{sn} + F \}; \quad (89)$$

where the new length scale for spin drift-diffusion is $l = L_{sn} = \sqrt{\frac{D_{nn}}{\phi_{nn}}} \cdot \frac{1}{2} \cdot \frac{1}{\phi_{nn}} (4 + 1 = L_{sn}^2)$ (the spin polarization decay is then governed by two length scales, L_{sn} , given by $l = L_{sn} = \sqrt{\frac{D_{nn}}{\phi_{nn}}}$, and spin ux

$$F = \frac{\exp(\phi_0 \frac{d\phi_{nn}}{dx} L_{sn})}{\sinh(\phi_{nn} L_{sn})} R \coth(\phi_{nn} L_{sn}); \quad (90)$$

To obtain ϕ_0 , one can still use Eq. (36), but with L_{sn} changed to L_{sn} and $\coth(\phi_{nn} L_{sn})$ changed to $\coth(\phi_{nn} L_{sn})$ ($\phi_{nn} L_{sn} = 2$). Similarly for the spin injection at large biases. Note that in the presence of magnetic impurities L_{sn} will be greatly reduced, so that $L_{sn} \ll 2$.

Although the inhomogeneous magnetic doping affects directly only the majority electrons, it modifies, through E_0 , transport of the minority holes as well, and thus the I-V characteristics of the junction. The hole current becomes

$$J_p = D_{pn} (\phi_0 R + \phi_0 \frac{d\phi_{nn}}{dx} L_{pn} + \phi_0^0); \quad (91)$$

where the first term describes drift of the nonequilibrium hole density by E_0 . Together with the continuity equation for hole current describing electron-hole recombination, the above equation, again in the limit of a constant $j_0 \gg 1$

leads to the hole current at $x = d_n$:

$$J_{pR} = D_{pn} \frac{p_R}{L_{pn}} - \frac{0R}{2} \frac{L_{pn}}{L_{pn}} + \coth \frac{w_n}{L_{pn}} ; \quad (92)$$

where we introduced an effective magnetic drift length $l=L_{pn} = \frac{p}{\omega} (\omega=4 + l=L_{pn}^2)$ (the two length scales for the hole density decay are L_{pn} given by $l=L_{pn} = l=L_{pn}^0=2$). Since $j_p = qJ_{pR}$, magnetic drift directly affects the I-V characteristics of the junction by modifying the hole minority current. It is in the combination with external bias $[p_R = \exp(V)]$ that the magnetic drift generates current. This effect could be used in electronic detection of magnetic field gradients.

Now we turn to the minority, p , region. Since the minority electron density can easily accommodate to spatial changes in n_p , no equilibrium electric field is needed to balance the magnetic drift force. The carrier and spin currents vanish at $E = 0$ for the equilibrium electron and spin densities, unlike in the n region considered above. From Eqs. (1)–(4), the drift-diffusion equations for the minority electrons and spin in the p region are obtained as

$$n^0 + E n^0 - \frac{0}{n_p} s^0 - \frac{\omega}{n_p} s = \frac{n}{L_{np}^2}; \quad (93)$$

$$s^0 + E s^0 - \frac{0}{n_p} n^0 - \frac{\omega}{n_p} n = \frac{s}{L_{np}^2} + \frac{s}{L_{1p}^2}; \quad (94)$$

Transport of minority carriers is thus coupled with the transport of spin. As a result, the electron current (and thus the I-V characteristics) will depend explicitly on nonequilibrium spin and, similarly, spin current will depend explicitly on nonequilibrium charge. Below we solve Eqs. (93) and (94) for the specific model of a linear n_p (that is, $n_p^0 = \text{constant}$) and in two limits of slow and fast spin relaxation. We will also neglect the electric field which is by about $n_L = N_d \ll 1$ smaller than the inverse of the typical decay length of the densities. Magnetic drift brings a new length scale, L_{np} , given by $l=L_{np} = \frac{p}{\omega} (\omega=4 + l=L_{np}^2)$. The density profiles then decay with two length scales, L_{np} , which are the inverse of $l=L_{np}^0=2$, depending on whether the diffusion is parallel (minus sign) or antiparallel (plus sign) to magnetic drift.

We now consider the limit of vanishing $l=L_{1p}$, which corresponds to slow spin relaxation (spin diffusion length is the largest length scale in the problem). We will not present the full density profiles here, only the final results for the electron and spin currents at the depletion layer boundary L , since they respectively determine the charge current in the junction and the spin injection through the depletion layer. The boundary conditions and the notation are the same as in Sec. (IIIA 1). The electron current at L , in analogy with Eq. (10), is $J_{nL} = (D_{np}=L_{np}) F_{np}$, where the modified flux

$$F_{np} = \frac{n_L \cosh(w_p=L_{np}) - n_p \cosh \frac{0}{n_p} w_p=2}{\sinh(w_p=L_{np})} - \frac{1}{2} \frac{0}{n_p} L_{np} - \frac{\sinh \frac{0}{n_p} w_p=2}{\sinh(w_p=L_{np})}; \quad (95)$$

If the magnetic drift vanishes, F_{np} becomes F_{np} . Since it is J_{nL} which gives the electron contribution to the total charge current through the junction, the charge current now explicitly depends on the nonequilibrium spin source s_p and the nonequilibrium spin at the depletion layer boundary, s_L . These contributions will be important if n_p will change on distances smaller than or comparable to L_{np} . Since J_{nL} is sensitive to the sign of $\frac{0}{n_p}$ (through the spin contribution), the charge current in a magnetic p - n junction could detect spatial changes in magnetic fields. If the junction serves as a solar cell or the base of a junction transistor⁹⁵, the nonequilibrium spin s_L alone will lead to charge current, in analogy with the term n_L leading to the usual solar cell current. In fact, both the nonequilibrium spin and carrier densities will be normally present when the junction is illuminated by light at $x = w_p$. The slope of n_p then either reduces or enhances the solar cell current, depending on the sign of $\frac{0}{n_p}$.

The spin current at L is $J_{sL} = (D_{np}=L_{np}) F_{sp}$, where

$$F_{sp} = \frac{s_L \cosh(w_p=L_{np}) - s_p \cosh \frac{0}{n_p} w_p=2}{\sinh(w_p=L_{np})} - \frac{1}{2} \frac{0}{n_p} L_{np} - \frac{s_p \sinh \frac{0}{n_p} w_p=2}{\sinh(w_p=L_{np})}; \quad (96)$$

When neglecting $l=L_{1p}$ in Eq. (94) the equations for electrons and spin become symmetric, so the spin current is obtained from the electron current by changing n_p to s_p and n_L to s_L , and vice versa. Also, in our limit of large L_{1p} ,

the effective spin diffusion length is $L_{sn} = L_{pn}$. In this limit the above equation reproduces J_{sL} from Eq. (15). If spin relaxation is slow, the spin current in a homogeneously spin split p region does not explicitly depend on the electron density. A finite ρ_{pn}^0 , however, couples the electron and the spin densities and the spin current acquires an explicit dependence on n_p and n_L . Spin injection is modified by magnetic drift too. If the n region remains magnetically homogeneous, the injected spin s_R can be obtained by equating J_{sL} calculated above and J_{sR} from Eq. (21). The result can be written as

$$s_R = s_0 s_n \frac{D_{np} L_{sn}}{D_{nn} L_{np}} \sinh(w_n = L_{sn}) F_{sp}^0; \quad (97)$$

where F_{sp}^0 is F_{sp} given by Eq. (96) with n_L and s_L calculated from Eqs. (32) and (33) using $s_R = 0$, that is, $n_L = n_{0L} [\exp(V) - 1]$ and $s_L = s_{0L} [\exp(V) - 1]$. Spin injection is modified in several ways. First, there are obvious modifications due to changes in the decay lengths, from L_{np} to L_{np} . Second, in our limit of $l = L_{1p} = 0$ there is no explicit contribution of n_p to s_R (see Eq. (36) with $\alpha_1 = \alpha_2$). Such an explicit dependence appears now because of the magnetic drift. Since the factor with n_p in Eq. (97) changes sign with ρ_{np}^0 , spin injection can be reduced or enhanced. Finally, the large bias spin extraction will be affected, since it now depends not only on s_{0L} but also on n_{0L} . The latter factor again enhances or reduces the large bias spin injection depending on the slope of n_p (more precisely, on the sign of $\rho_{np}^0 s_{0L}$).

In the opposite limit of fast spin relaxation (which is perhaps more realistic in magnetically doped samples under consideration) one can assume for the spin to follow the local carrier density changes: $s = \rho_{0n}$. Only the drift-diffusion equation for electrons, Eq. (93), needs to be solved in this case. To simplify the discussion, we further assume that the homogeneous part of the magnetic spin splitting is large, and $\rho_0 \gg 1$, with $\rho_0^0 = 0$. The carrier and spin currents have the same magnitude, only the sign can differ if $\rho_0 = -1$. It thus suffices to look at the carrier current. In analogy with the previous case, the spin current is determined by F_{np} , which now reads

$$F_{np} = n_L \coth(w_p = L_{np}) \rho_{np}^0 L_{np} = 2 \frac{\exp(\rho_0 w_p = 2)}{\sinh(w_p = L_{np})}; \quad (98)$$

The spin current and the spin injection (that is, s_R) are then given as in the previous limit of slow spin relaxation, but with $F_{sn} = \rho_{np}^0 F_{np}$. As in the case of slow spin relaxation, here too the I-V curve becomes explicitly dependent on magnetic drift. The strength of the magnetic drift is determined by the parameter $\rho_{np}^0 L_{np}$, while the sign (whether it will enhance or reduce the charge current) on the sign of ρ_{np}^0 . The solar cell current coming from n_p depends exponentially on ρ_{np}^0 . The same applies to spin injection.

V. SUMMARY AND CONCLUSIONS

We have studied spin-polarized bipolar transport in magnetic p-n junctions under the general conditions of applied bias and externally injected (source) spin. We have introduced a model, by generalizing the successful Shockley model of nonmagnetic p-n junctions, to include spin-split bands and nonequilibrium spin. The model is valid only at low injection (small biases), although it shows the trends of what to expect at large biases as well. Our theory gives the carrier and spin density profiles in the bulk regions (away from the depletion layer), and explicitly formulates the boundary conditions for the densities at the depletion layer. In analogy with the original Shockley model we employ the condition of (quasi) thermal equilibrium across the depletion layer even when a bias is applied and a nonequilibrium spin is injected. However, the spin polarized case requires an additional condition to obtain all the relevant input parameters. This condition we formulate in terms of the continuity of the spin current across the depletion layer. The obtained boundary conditions allow us to generalize the standard diode formulas to the case of spin-polarized magnetic diodes, resulting in a new formulation of the I-V characteristics. Although to explain the physics of bipolar spin-polarized transport we use spin polarized electrons only, we also give all the formulas needed to calculate the I-V curves for spin polarized holes as well (in the Appendix, where we also show how the equilibrium properties of p-n junctions are modified in the presence of spin-split bands).

We have applied our theory to several cases which we believe are important for spintronics. We demonstrate that only nonequilibrium spin can be injected across the depletion layer. Effective spin injection from a magnetic into a nonmagnetic region, without a source spin, is not possible at small biases. We show how this claim is relaxed at large biases, which build up a nonequilibrium spin in the magnetic majority region, and then inject this spin into the nonmagnetic minority region. Similarly, we demonstrate that spin can be extracted at large forward biases from the nonmagnetic majority region to the magnetic minority one. We also study spin injection by the minority

carriers to the majority region. Physically, this process can be described as spin pumping, since the resulting accumulation/amplification of spin in the majority region depends on the spin current of the minority carriers. The accumulated spin can be greater than the source spin, which in effect is a spin amplification. A realization of the spin-voltaic effect is found at the interface (here the depletion layer) between the minority magnetic region (p) and the nonmagnetic but spin-polarized majority region. The spin-voltaic effect is demonstrated by the generation of charge current by nonequilibrium spin (at no applied bias). This is also a spin-valve effect, since the direction of the charge current can be reversed by reversing an applied magnetic field. The spin induced nonequilibrium charge density is also the basis for the spin capacitance of the spin-polarized junctions⁵³ as well as for the spin and magnetic field dependent charge capacitance of magnetic p-n junctions.⁹⁵ Next we have studied (source) spin injection by the biasing electrode and shown that this is not a very effective means of spin injection, at least for a simple model considered. Finally, we demonstrated that if the neutral regions have nonequilibrium band spin splitting, the resulting magnetic drift can significantly affect both the I-V characteristics of the junction and the junction spin injection capabilities.

Our theory is general enough to be applicable to various semiconductor spintronic devices operating under the conditions of small injection and nondegenerate carrier statistics. While we have already demonstrated the extensive generality of the theory by applying it to a large number of specific model device simulations, we envisage many more potential spintronic junction devices where our models will be useful. Such devices can be, for example, bipolar spin junction transistors⁹⁵ or spin thyristors, with great technological potentials, and where charge currents (and their amplification) can be controlled not only by bias, but also by nonequilibrium spin and magnetic field. However, to apply the theory to realistic device structures, many physical aspects of the model will need to be modified. In many cases the spin states of the carriers are not simple spin doublets, but rather multiplets, as a result of the spin-orbit coupling. In addition, the electron-hole recombination is, in general, spin selective, so if both electrons and holes are spin polarized, more realistic models for the recombination need to be introduced. Furthermore, carrier recombination and spin relaxation depend on the carrier density, an effect which may be found important if ferromagnetic semiconductors are employed. Other possible additions to the model may include a realistic treatment of spin relaxation (and carrier recombination) in the depletion layer and finite spin relaxation at the contact electrodes. Structural modifications may include inhomogeneous magnetic doping (or inhomogeneous magnetic fields) also in the bulk regions, and schemes based on two or three dimensional spin bipolar transport. Since, at the moment, there is a lack of experimental understanding of bipolar spin transport, theoretical modeling (both analytical as presented here or numerical, which is of greater applicability, as reported in Refs. 52,53,54) is particularly important. We believe that although quantitative aspects of spin-polarized bipolar transport may be seriously modified, our theory captures the essential physics and the predicted phenomena are robust enough to be present in more realistic situations.

Acknowledgments

We would like to thank Prof. E. I. Rashba for useful discussions. This work was supported by DARPA, the US ONR, and the NSF.

APPENDIX A : EQUILIBRIUM PROPERTIES OF MAGNETIC P-N JUNCTIONS

To study equilibrium properties of magnetic p-n junctions we consider both electrons and holes spin polarized. Denote the electron and hole spin densities as s_n and s_p , and reserve the second subscript (if needed) to denote the region. Symbol 0 denotes the equilibrium values. As in the main text, the energies (potentials) are given in the units of $k_B T$ ($k_B T = q$). Further, denote as ϵ_n and ϵ_p the spin band splittings of the conduction and valence bands. We adopt the convention that ϵ_n (ϵ_p) is positive when the spin up electrons (holes) have a lower energy than those in the spin down states. Both electrons and holes are assumed in thermal equilibrium, obeying nondegenerate Boltzmann statistics.

The equilibrium carrier densities obey the law of mass action, now reading

$$n_0 p_0 = n_i^2 \cosh(\epsilon_n) \cosh(\epsilon_p); \quad (A1)$$

As a result, the minority carrier densities (electrons in the p region and holes in the n region) are

$$n_{0p} = \frac{n_i^2}{N_a} \cosh(\epsilon_{np}) \cosh(\epsilon_{pp}); \quad (A2)$$

$$p_{0n} = \frac{n_i^2}{N_d} \cosh(\epsilon_{pn}) \cosh(\epsilon_{nn}); \quad (A3)$$

Similarly, the corresponding equilibrium spin densities are

$$s_{0,np} = \frac{n_i^2}{N_a} \sinh(\eta_{np}) \cosh(\eta_{pp}); \quad (\text{A } 4)$$

$$s_{0,pn} = \frac{n_i^2}{N_d} \sinh(\eta_{pn}) \cosh(\eta_{nn}); \quad (\text{A } 5)$$

so that the equilibrium spin polarizations of electrons and holes are $\eta_{0n} = \tanh(\eta_n)$ and $\eta_{0p} = \tanh(\eta_p)$. The built-in voltage, which is the electrostatic potential drop across the depletion layer depends on the band splittings (thus on the equilibrium spin polarizations):

$$V_b = \ln \frac{N_a N_d}{n_i^2} - \ln [\cosh(\eta_{pp}) \cosh(\eta_{nn})]; \quad (\text{A } 6)$$

The built-in voltage is slightly reduced by the spin splitting. Note that only the band splittings of the majority carriers affect the built-in field. The reason is that the chemical potentials in the bulk regions (considered separately) depend only on η_{nn} and η_{pp} :

$$\eta_{0n} = \eta_i + \ln \frac{N_d}{n_i} - \ln \cosh(\eta_{nn}); \quad (\text{A } 7)$$

$$\eta_{0p} = \eta_i - \ln \frac{N_a}{n_i} + \ln \cosh(\eta_{pp}); \quad (\text{A } 8)$$

Here η_i is the chemical potential for the intrinsic (undoped) and unpolarized case. In making a junction, the built-in field arises upon equilibrating the two chemical potentials: $V_b = \eta_{0n} - \eta_{0p}$. The band splitting does not affect the nondegeneracy of the carrier statistics, since the distance between the chemical potential and the lower conduction (upper valence) spin band does not change with η at large η .

APPENDIX B: SPIN POLARIZED HOLES

Spin polarization of holes can be treated separately from that of electrons, since, in our model, electron and hole transport are independent (only minority diffusion is considered), and the electron-hole recombination is spin independent (in our simplified picture electrons of one spin can recombine with holes of either spin). Inclusion of spin polarization of holes into our theory then amounts to simple notation exchange, p with n and L with R . For completeness, we present all the important formulas which are needed to obtain the charge current contribution by spin polarized holes. Since this is a separate section from the main text, we adopt the same notation for the hole spin as we had before for electrons, without using more elaborate set of indexes. The hole spin density (only in this section) is s and the hole spin polarization is η . All the other symbols retain their original meaning.

In analogy with Eq. (41), the hole charge current is

$$j_p = j_{0p} + j_{1p} + j_{2p}; \quad (\text{B } 1)$$

where

$$j_{0p} = j_{gp} e^{\eta_{0p}} - 1; \quad (\text{B } 2)$$

$$j_{1p} = j_{gp} e^{\eta_{0p}} \left[L \frac{\eta_{0R}}{1} - \frac{\eta_{0L}}{2} \right]; \quad (\text{B } 3)$$

$$j_{2p} = j_{gp} \frac{1}{\cosh(\eta_{pn} = L_{pn})} \frac{p_n}{p_{0R}}; \quad (\text{B } 4)$$

The hole generation current is

$$j_{gp} = \frac{q D_{pn}}{L_{pn}} p_{0R} \coth(\eta_{pn} = L_{pn}); \quad (\text{B } 5)$$

The (now majority) hole spin, in analogy with Eq. (36) can be expressed as

$$s_L = \eta_{0p} s_p + \eta_{1p} s_n + \eta_{2p} \frac{p_n}{p_{0R}} p_n - \eta_{0R} e^{\eta_{0R}} - 1; \quad (\text{B } 6)$$

where the geometric/transport factors are

$$0 = 1 = \cosh(w_p = L_{sp}); \quad (B 7)$$

$$1 = \frac{D_{pn}}{D_{pp}} \frac{L_{sp}}{L_{sn}} \frac{\tanh(w_p = L_{sp})}{\sinh(w_n = L_{sn})}; \quad (B 8)$$

$$2 = \frac{D_{pn}}{D_{pp}} \frac{L_{sp}}{L_{pn}} \frac{\tanh(w_p = L_{sp})}{\sinh(w_n = L_{pn})}; \quad (B 9)$$

$$3 = 2 \cosh(w_n = L_{pn}); \quad (B 10)$$

Finally, the (now minority) hole density and spin in the n side of the depletion layer are

$$p_R = p_{0R} e^{V} \left[1 + \frac{L}{1} \frac{0R}{1} \frac{0L}{2} \right]; \quad (B 11)$$

$$s_R = s_{0R} e^{V} \left[1 + \frac{L}{0R} \frac{1}{1} \frac{0R}{1} \frac{0L}{2} \right]; \quad (B 12)$$

Physical consequences of the spin polarization of holes in bipolar transport are in complete analogy with the physics discussed in the main text where only spin-polarized electrons are considered. In particular, the hole charge current j_p from Eq. (B 1) needs to be substituted to the total charge current formula, Eq. (47). In many cases, however, one can realistically treat only one carrier type as spin polarized. If, for example, holes have a very short spin lifetime (or small diffusivity), their spin polarization (even their contribution per se) does not need to be considered. The exceptional cases are the large bias spin-polarized transport and magnetic drift in the bulk regions, treated in Secs. IV E and IV F, respectively, in which electron and hole transport can be strongly coupled.

APPENDIX C : MAJORITY ELECTRON DRIFT AND DIFFUSION

The spin profile in the n region is affected by the electric field and charge neutrality, as described by Eq. (79). Assuming the same boundary conditions for spin as in Sec. III A 2, that is, $s(d_h) = s_R$ and $s(w_n) = s_n$, and the boundary conditions for holes $p(d_h) = p_R$ and $p(w_n) = 0$ (ohmic contact), the solution to Eq. (79) can be written in the form analogous to Eq. (18):

$$s = e^{E(x - d_n)/2} \left(\hat{s}_R \cosh(s_E) + F_{sE} \sinh(s_E) \right) + 0_n \hat{p}; \quad (C 1)$$

We now describe the new notation. The effective deviations from the equilibrium of spin and hole densities are

$$\hat{s}_R = s_R - A_{0n} p_R [1 + E \coth(w_n = L_{pn})]; \quad (C 2)$$

$$\hat{p} = A [p + E (L_{pn} = D_{pn}) J_p]; \quad (C 3)$$

where $E = E = 2L_{pn}$ measures the strength of the electric field for drifting spin, $= \frac{P}{(1=L_{pn}^2 - 1=L_{sn}^2)}$ (the singular case of $= 0$ is excluded from the solution), and $1=A = (L_{sn})^2 (1 - \frac{2}{E})$. The normalized flux is

$$F_{sE} = \frac{\hat{s} \cosh(w_n = L_{sE}) + \hat{s}_n \exp(E w_n/2)}{\sinh(w_n = L_{sE})}; \quad (C 4)$$

introducing a length scale L_{sE} for electric spin drift: $1=L_{sE} = \frac{P}{(E^2=4 + 1=L_{sn}^2)}$, which is also used to define $s_E(x - d) = L_{sE}$. This length scale was already introduced in Refs. 55,56,94. The new effective spin density

$$\hat{s}_n = s_n - \frac{A_{0n} p_R E}{\sinh(w_n = L_{pn})}; \quad (C 5)$$

Finally, the hole density profile p is obtained by solving independently for hole diffusion, Eq. (80). For completeness we show the result:

$$p = p_R \cosh(p_n) + F_{pn} \sinh(p_n); \quad (C 6)$$

where $p_n(x - d) = L_{pn}$ and

$$F_{pn} = p_R \coth(w_n = L_{pn}); \quad (C 7)$$

The hole current is then $J_p = -D_{pn} p^0$.

The importance of electric drift for the majority electron spin transport is in aiding the spin injection through the depletion layer, from the majority magnetic to the minority nonmagnetic region. To see how spin can be injected through the depletion layer we need to know the spin current at the depletion layer boundary. The spin current profile is $J_s = -D_{nn}(sE + s^0)$, where s is given by Eq. (C1). The spin current at $x = d_n$ is

$$\begin{aligned} J_{sR} = & D_{nn} \left(s_{0n} + \frac{1}{2} s_R \right) E \\ & + \frac{D_{nn}}{L_{SE}} \frac{s_R \cosh(w_n = L_{SE})}{\sinh(w_n = L_{SE})} s_R \exp(E w_n = 2) \\ & + \frac{D_{nn}}{L_{pn}} s_{0n} p_R A \coth \frac{w_n}{L_{pn}} \\ & + \frac{D_{nn}}{L_{SE}} s_{0n} p_R A \coth \frac{w_n}{L_{SE}} ; \end{aligned} \quad (C8)$$

where we neglected terms of order $E D_{nn} p_R = L_{pn}$. For most practical cases in magnetic p-n junctions the electric field at low injection can be neglected, so that $E L_{pn} \ll E L_{SE} \ll 1$. Then $L_{SE} \approx L_{sn}$, $1 = L_{pn}$, and $A \approx (L_{pn} = L_{sn})^2$. Since E is of order $p_R = L_{pn}$, the contribution to the spin current (and thus to spin injection) from the hole density is negligible, since in the considered limit $A \ll 1$. If s_R is greater than, say, $10^{-3} N_d$, then also the contribution from the electric drift can be neglected (not limited to the above limit), verifying our theory in the main text. If, however, the source spin is small, and there is appreciable forward bias, the electric drift has to be taken into account for describing spin injection across the depletion layer. This is done in Sec. (IV E).

-
- ¹ S. Das Sarma, J. Fabian, X. Hu, and I. Zutic, IEEE Transaction on Magnetics 36, 2821 (2000); Superlattice Microsc. 27, 289 (2000); Solid State Commun. 119, 207 (2001).
 - ² D. Loss and D. P. DiVincenzo, Phys. Rev. A 57, 120, 1998.
 - ³ X. Hu and S. Das Sarma, Phys. Rev. A 61, 062301 (2000).
 - ⁴ F. Meier and B. P. Zakharchenya (eds), Optical Orientation (North-Holland, New York 1984).
 - ⁵ A. G. Aronov, Sov. Phys. Semicond. 10, 698 (1976).
 - ⁶ M. Oestreich, J. Hubner, D. Hagele, P. J. Klar, W. Heimbrodt, W. W. Ruhle, D. E. Ashenford, and B. Lunn, Appl. Phys. Lett. 74, 1251 (1999).
 - ⁷ R. Fiederling, M. Klemm, G. Reuscher, W. Ossau, G. Schmidt, A. W. Wegmann, and L. W. Molenkamp, Nature 402, 787 (1999).
 - ⁸ Y. Ohno, D. K. Young, B. Beschoten, F. Matsukura, H. Ohno, and D. D. Awschalom, Nature 402, 790 (1999).
 - ⁹ B. T. Jonker, Y. D. Park, B. R. Bennett, H. D. Cheong, G. Kioseoglou, and A. Petrou, Phys. Rev. B 62, 8180 (2000).
 - ¹⁰ P. R. Hammar, B. R. Bennett, M. J. Yang, M. Johnson, Phys. Rev. Lett. 83, 203 (1999).
 - ¹¹ H. J. Zhu, M. Ramsteiner, H. Kostial, M. W. Asselmeier, H.-P. Schonherr, and K. H. Ploog, Phys. Rev. Lett. 87, 016601 (2001).
 - ¹² V. Dediu, M. Murgu, F. C. Matocotta, C. Taliani, and S. Barbanera, Solid State Commun. 122, 181 (2002).
 - ¹³ C.-M. Hu, J. Nitta, A. Jensen, J. B. Hansen, and H. Takayanagi, Phys. Rev. B 63, 125333 (2001).
 - ¹⁴ P. R. Hammar and M. Johnson, Appl. Phys. Lett. 79, 2591 (2001).
 - ¹⁵ A. T. Hanbicki, B. T. Jonker, G. Itskos, G. Kioseoglou, and A. Petrou, Appl. Phys. Lett. 80, 1240 (2002).
 - ¹⁶ V. F. Motsnyi, V. I. Safarov, J. de Boeck, J. Das, W. Van Roy, E. Goovaerts, and G. Borghs, preprint cond-mat/0110240.
 - ¹⁷ S. van Dijken, X. Jiang, and S. S. P. Parkin, Appl. Phys. Lett. 80, 3364 (2002).
 - ¹⁸ J. Fabian and S. Das Sarma, J. Vac. Sci. Technol. B 17, 1780 (1999).
 - ¹⁹ D. Hagele, M. Oestreich, and W. W. Ruhle, N. Nestle, and K. Eberl, Appl. Phys. Lett. 73, 1580 (1998).
 - ²⁰ J. M. Kikkawa and D. D. Awschalom, Nature, 139 (1999).
 - ²¹ I. Malajovich, J. J. Berry, N. Samarth, and D. D. Awschalom, Nature 411, 770 (2001).
 - ²² Th. Guber, M. Klemm, R. Fiederling, G. Reuscher, W. Ossau, G. Schmidt, L. W. Molenkamp, and A. Wegmann, Appl. Phys. Lett. 78, 1101 (2001).
 - ²³ M. Kohda, Y. Ohno, K. Takamura, F. Matsukura, and H. Ohno, Jpn. J. Appl. Phys. 40, L1274 (2001).
 - ²⁴ E. Johnston-Halperin, D. Lofgreen, R. K. Kawakami, D. K. Young, L. Coldren, A. C. Gossard, and D. D. Awschalom, Phys. Rev. B 65 041306 (2002).
 - ²⁵ A. Hirohata, Y. B. Xu, C. M. Guertler, J. A. C. Bland, and S. N. Holmes, Phys. Rev. B 63, 104425 (2001).
 - ²⁶ A. F. Isakovic, D. M. Carr, J. Strand, B. D. Schultz, C. J. Palmstrom, and P. A. Crowell, Phys. Rev. B 64, 161304 (2001).
 - ²⁷ G. Schmidt, G. Richter, P. G. Rabbs, C. Gould, D. Ferrand, and L. W. Molenkamp, Phys. Rev. Lett. 87, 227203 (2001).
 - ²⁸ S. D. Ganichev, E. L. Ivchenko, S. N. Danilov, J. Erum, W. Wegscheider, D. Weiss, and W. Prettl, Phys. Rev. Lett. 86, 4358 (2001).
 - ²⁹ H. Munekata, H. Ohno, S. von Molnar, A. Segmuller, L. L. Chang, and L. Esaki, Phys. Rev. Lett. 63, 1849 (1989).

- ³⁰ H. Ohno, H. Muneoka, T. Penney, S. von Molnar, and L. L. Chang, Phys. Rev. Lett. 68, 2664 (1992).
- ³¹ H. Ohno, Science 281, 951 (1998).
- ³² A. Van Esch, L. Van Bockstal, J. De Boeck, G. Verbanck, A. S. van Steenberghe, P. J. Wellmann, B. Grietens, R. Bogaerts, F. Herlach, and G. Borghs, Phys. Rev. B 56, 13103 (1997).
- ³³ H. Krenn, K. Kaltenegger, T. Dietl, J. Spalek, and G. Bauer, Phys. Rev. B 39, 10 918 (1989).
- ³⁴ S. Koshihara, A. Oiwa, M. Hirasawa, S. Katsumoto, Y. Iye, S. Umano, H. Takagi, and H. Muneoka, Phys. Rev. Lett. 78, 4617 (1997).
- ³⁵ H. Ohno, D. Chiba, F. Matsukura, T. Omiya, E. Abe, T. Dietl, Y. Ohno, and K. Ohtani, Nature 408, 944 (2000).
- ³⁶ Y. D. Park, A. T. Hanbicki, S. C. Erwin, C. S. Hellberg, J. M. Sullivan, J. E. Mattson, T. F. Ambrose, A. Wilson, G. Spanos, and B. T. Jonker, Science 295, 651 (2002).
- ³⁷ T. Slupinski, H. Muneoka, and A. Oiwa, preprint cond-mat/0201363.
- ³⁸ G. A. Medvedkin, T. Ishibashi, T. Nishi, K. Hayata, Y. Hasegawa, and K. Sato, Jpn. J. Appl. Phys. 39, L949 (2000).
- ³⁹ M. L. Reed, N. A. Elmasry, H. H. Stadler, Appl. Phys. Lett. 79, 3473 (2001).
- ⁴⁰ N. Theodoropoulou, A. F. Hebard, M. E. Overberg, C. R. Abemathy, S. J. Pearton, S. N. G. Chu, and R. G. Wilson, preprint cond-mat/0201492.
- ⁴¹ Y. Matsumoto, M. Murakami, T. Shono, T. Hasegawa, T. Fukumura, M. Kawasaki, P. Ahmet, T. Chikyow, S. Koshihara, and H. Koinum, Science 291, 854 (2001).
- ⁴² G. Schmidt, D. Ferrand, L. W. Molenkamp, A. T. Filip and B. J. van Wees, Phys. Rev. B 62, 4790 (2000).
- ⁴³ E. I. Rashba, Phys. Rev. B 62, 16 267 (2000).
- ⁴⁴ D. L. Smith and R. N. Silver, Phys. Rev. B 64 045323 (2001).
- ⁴⁵ A. Fert and H. Jares, Phys. Rev. B, 64, 184420 (2001).
- ⁴⁶ C. M. Hu and T. Matsuyama, Phys. Rev. Lett. 87, 066803 (2001).
- ⁴⁷ R. H. Silsbee, Phys. Rev. 63, 155305 (2001).
- ⁴⁸ E. I. Rashba, Appl. Phys. Lett. 80, 2329 (2002).
- ⁴⁹ S. Das Sarma, J. Fabian, X. Hu, and I. Zutic, 58th DRC (Device Research Conference) Conference Digest, p. 95-8 (IEEE, Piscataway, 2000); preprint cond-mat/0006369.
- ⁵⁰ H. X. Tang, F. G. Monzon, R. Lifshitz, M. C. Cross, and M. L. Roukes, Phys. Rev. B 61, 4437 (2000).
- ⁵¹ M. E. Flatte and J. M. Byers, Phys. Rev. Lett. 84, 4220 (2000).
- ⁵² I. Zutic, J. Fabian, and S. Das Sarma, Phys. Rev. B 64, 121201 (2001).
- ⁵³ I. Zutic, J. Fabian, and S. Das Sarma, Appl. Phys. Lett. 79, 1558 (2001).
- ⁵⁴ I. Zutic, J. Fabian, and S. Das Sarma, Phys. Rev. Lett. 88, 066603 (2002).
- ⁵⁵ Z. G. Yu and M. E. Flatte, preprint cond-mat/0201425.
- ⁵⁶ I. Martin, preprint cond-mat/0201481.
- ⁵⁷ I. Zutic, J. Fabian, and S. Das Sarma, preprint cond-mat/0205177.
- ⁵⁸ S. Datta and B. Das, Appl. Phys. Lett. 56 665 (1990).
- ⁵⁹ S. Gardelis, C. G. Smith, C. H. W. Barnes, E. H. Linfield, and D. A. Ritchie, Phys. Rev. B 60, 7764 (1999).
- ⁶⁰ Th. Schapers, J. Nitta, H. B. Heersche, and H. Takayanagi, Phys. Rev. B 64, 125314 (2001).
- ⁶¹ E. I. Rashba, Sov. Phys. Solid State 2, 1109 (1960).
- ⁶² Y. A. Bychkov and E. I. Rashba, J. Phys. C 17, 6039 (1984).
- ⁶³ J. Carlos Egues, Phys. Rev. Lett. 98, 4578 (1998).
- ⁶⁴ A. E. de Andrada e Silva and G. C. La Rocca, Phys. Rev. B 59, 15 583 (1999).
- ⁶⁵ G. Kirczenow, Phys. Rev. B 63, 054422 (2001).
- ⁶⁶ Y. Guo, J.-Q. Lu, B.-L. Gu, and Y. Kawazoe, Phys. Rev. B 64, 155312 (2001).
- ⁶⁷ A. A. Kiselev and K. W. Kim, Appl. Phys. Lett. 78, 775 (2001).
- ⁶⁸ A. L. Efros, E. I. Rashba, and M. Rosen, Phys. Rev. Lett. 87, 206601 (2001).
- ⁶⁹ T. Matsuyama, C. M. Hu, D. Gundler, G. Meier, and U. Merkt, Phys. Rev. B 65, 155322 (2002).
- ⁷⁰ M. G. Overmire, D. Boese, U. Zolick, and C. Schroll, preprint cond-mat/0108373.
- ⁷¹ J. W. Robel, T. Dietl, K. Fronc, A. Lusakowski, M. C. Zeczott, G. G. Rabecki, R. Hey, and K. H. Ploog, Physica E 10, 91 (2001).
- ⁷² V. M. Ramaglia, V. Cataudella, G. De Filippis, C. A. Perroni, F. Ventriglia, preprint cond-mat/0203569.
- ⁷³ I. Zutic and S. Das Sarma, Phys. Rev. B 60, 16 322 (1999).
- ⁷⁴ A. G. Petukhov, Appl. Surf. Sci. 123/124, 385 (1998).
- ⁷⁵ M. E. Flatte and G. Vignale, Appl. Phys. Lett. 78, 1273 (2001).
- ⁷⁶ D. Frustaglia, M. Hentschel, and K. Richter, Phys. Rev. Lett. 87, 256602, (2001).
- ⁷⁷ S. K. Joshi, D. Sahoo, and A. M. Jayannavar, Phys. Rev. B 64, 075320 (2001).
- ⁷⁸ B. K. Nikolic and J. K. Freericks, preprint cond-mat/0111144.
- ⁷⁹ M. I. Dyakonov and V. I. Perel', Phys. Lett. 35 A, 459 (1971).
- ⁸⁰ M. I. Dyakonov and V. I. Perel', JETP Lett. 13, 467 (1971).
- ⁸¹ J. E. Hirsch, Phys. Rev. Lett. 83, 1834 (1999).
- ⁸² R. D. R. Bhat and J. E. Sipe, Phys. Rev. Lett. 85, 5432 (2000).
- ⁸³ A. B. Rataas, Y. Tserkovnyak, G. E. W. Bauer, and B. I. Halperin, preprint cond-mat/0205028.
- ⁸⁴ At low temperature $\rho > 500$ in $(\text{Cd}_{0.95}\text{Mn}_{0.05}\text{Se})$. In: See T. Dietl, Handbook of Semiconductors Vol. 3, edited by T. S. Moss and S. Mahajan, p. 1279 (North-Holland, New York, 1994).
- ⁸⁵ R. H. Silsbee, Bull. Magn. Reson. 2, 284 (1980).
- ⁸⁶ M. Johnson and R. H. Silsbee, Phys. Rev. Lett. 55, 1790 (1985).

- ⁸⁷ W. Shockley, *Electrons and Holes in Semiconductors* (D. Van Nostrand, Princeton, 1950).
- ⁸⁸ S. Tiwari, *Compound Semiconductor Device Physics* (Academic Press, San Diego, 1992).
- ⁸⁹ Typically one region would be nonmagnetic (or only weakly magnetic). This would be the region where the nonequilibrium spin would be generated and transported to the depletion layer. If the region were magnetic, such transport could be hindered by fast spin relaxation.
- ⁹⁰ N. W. Ashcroft and N. D. Mermin, *Solid State Physics* (Sounders 1976).
- ⁹¹ M. I. Dyakonov and V. I. Perel', *JETP Lett.* 13, 144 (1971).
- ⁹² This is an accurate approximation for low bias, as shown a posteriori by comparing our analytical model with the self-consistent numerical solution in Ref. 54.
- ⁹³ Y. Q. Jia, R. C. Shi, S. Y. Chou, *IEEE Transactions on Magnetics* 32, 4709 (1996).
- ⁹⁴ I. Zutic, unpublished.
- ⁹⁵ J. Fabian, I. Zutic, and S. Das Sarma, unpublished.